Improving Generalization of Neural Combinatorial Optimization for Vehicle Routing Problems via Test-Time Projection Learning

Yuanyao Chen[1,2*]**, Rongsheng Chen**[1,2,3*]**, Fu Luo**[1,2]**, Zhenkun Wang**[1,2†]

[1] School of Automation and Intelligent Manufacturing,
Southern University of Science and Technology, Shenzhen, China,
[2] Guangdong Provincial Key Laboratory of Fully Actuated System Control Theory and Technology,
Southern University of Science and Technology, Shenzhen, China,
[3] Peng Cheng Laboratory, Shenzhen, China,
12433020@mail.sustech.edu.cn, chenrs1017@gmail.com,
luof2023@mail.sustech.edu.cn, wangzhenkun90@gmail.com

Abstract

Neural Combinatorial Optimization (NCO) has emerged as a promising learning-based paradigm for addressing Vehicle Routing Problems (VRPs) by minimizing the need for extensive manual engineering. While existing NCO methods, trained on small-scale instances (e.g., 100 nodes), have demonstrated considerable success on problems of similar scale, their performance significantly degrades when applied to large-scale scenarios. This degradation arises from the distributional shift between training and testing data, rendering policies learned on small instances ineffective for larger problems. To overcome this limitation, we introduce a novel learning framework driven by Large Language Models (LLMs). This framework learns a projection between the training and testing distributions, which is then deployed to enhance the scalability of the NCO model. Notably, unlike prevailing techniques that necessitate joint training with the neural network, our approach operates exclusively during the inference phase, obviating the need for model retraining. Extensive experiments demonstrate that our method enables a backbone model (trained on 100-node instances) to achieve superior performance on large-scale Traveling Salesman Problems (TSPs) and Capacitated Vehicle Routing Problems (CVRPs) with up to 100K nodes from diverse distributions. The source code can be found in https://github.com/CIAM-Group/TTPL.

1 Introduction

The vehicle routing problem (VRP) is prevalent in critical domains such as transportation [1], logistics [2], and supply chain management [3]. However, due to the NP-hard nature, solving a VRP can be complex and time-consuming [4]. While traditional exact and heuristic methods can yield optimal or near-optimal solutions, their high computational cost and dependence on domain expertise consequently diminish their feasibility for real-world deployment.

In recent years, neural combinatorial optimization (NCO) has emerged as a promising approach for solving VRP [5]. It utilizes neural networks to learn problem-solving strategies directly from the VRP instances, minimizing the need for algorithms designed by experts. Once trained, these neural networks can efficiently generate solutions for new instances at a low computational cost. Therefore,

---

[*]Equal contributors
[†]Corresponding author

NCO methods demonstrate potential advantages in tackling limitations of traditional methods and exhibit promising performance in solving small-scale VRPs [6–9].

However, due to the different distributions between small and large-scale instances, the effectiveness of existing approaches degrades substantially when it comes to large-scale problems (e.g., problems with more than 1K nodes), thereby severely limiting their practical capability. To address the scalability issue, some attempts have been devoted to training NCO models on larger VRP instances (i.e., instances with 500 nodes) [10, 11]. However, the existing supervised learning (SL) and reinforcement learning (RL) both show their shortcomings when training on large-scale VRP instances. SL lacks sufficient labels (e.g., high-quality solutions) while RL suffers from extremely sparse rewards.

Consequently, current methods focus on training a model on small-scale instances and generalizing to large-scale scenarios via decomposition or local policy [12–15]. The decomposition-based method first simplifies large-scale problems to a series of subproblems. Subsequently, a solver trained on the small-scale instances can be utilized to construct a partial solution of the subproblems [16–18]. However, the scope of the decomposition often requires manual tuning, and even decomposing the problem could change its property, and thus damage the optimality of the solving algorithm. Another effort is local policy-based methods [14, 15]. It first reduces the search space to a small candidate subgraph at each construction step, typically based on the Euclidean distance to the last visited node. The next node is decided by the original policy or a local policy.

However, the distribution of selected subgraphs often differs from training instances, which significantly impairs the model's scalability. Current methods employ a projection technique to effectively transform these varied input distributions into a uniform distribution encountered during training [15, 13, 19]. Nevertheless, existing strategies require integration with the model training to ensure effectiveness during testing. Meanwhile, these manually designed strategies heavily rely on specialized domain expertise, thereby limiting their adaptability.

To address this challenge, we propose a novel learning framework called Test-Time Projection Learning (TTPL), driven by the Large Language Model (LLM), to design an efficient projection strategy. In particular, we utilize the LLM to learn the correlation between the input subgraph and training instances, thereby developing projection strategies that enhance model generalization. Different from existing works, our approach can be directly applied in the inference phase, does not need to train a model from scratch. Moreover, we propose a Multi-View Decision Fusion (MVDF) module to improve model generalization. Specifically, we perform data augmentation on the subgraph to generate multiple views. These views are subsequently processed by the model, with each view yielding a distinct node selection probability. Finally, these probabilities are aggregated, and the node with the highest resulting confidence score is selected.

Comprehensive experiments are conducted on both synthetic and real-world benchmarks for the TSP and CVRP. The results demonstrate that our proposed distribution adapter enables the base model, pre-trained on small-scale instances (e.g., 100 nodes), to achieve superior performance on the majority of large-scale VRP test instances without requiring additional fine-tuning. Our ablation study validates the effectiveness of the designed projection strategy.

2 Related Work

Existing NCO methods can be categorized into constructive [20–25] and non-constructive [26–29]. This paper mainly focuses on the constructive method; a detailed review of the non-constructive method and other LLM-based methods can be found in the Appendix. A.

2.1 Direct Generalization

This kind of method often trains neural networks on small-scale instances and generalizes them to large-scale instances. It is mostly known as the construction-based methods that predict an approximate solution in an autoregressive manner. Early studies demonstrate that neural models trained with SL or RL can reach promising performance on small-scale instances [30–32]. Moreover, [6, 33] propose to use the Transformer architecture [34] to design powerful attention-based models to solve VRPs. Subsequently, various Transformer-based approaches have been developed with different strengths [35–41]. Meanwhile, many studies focus on improving model performance on large-scale

VRPs [42]. In which [42] and [18] train the model with SL on 100-node and exhibit generalization ability to 1K nodes. Specifically, BQ [42] modifies the Markov Decision Process (MDP) to efficiently leverage the symmetries of combinatorial optimization problems (COPs). LEHD [18] develops a light encoder and heavy decoder structure to reach the same result. Nevertheless, the training distribution of 100-node instances drastically differs from the large-scale instances; the trained model usually performs poorly when tested on this large-scale scenario. Consequently, several attempts have trained models on larger-scale instances with up to 500 nodes [43, 11, 38, 10] or even directly training on the large-scale [44] (up to 100K-nodes). However, these approaches introduce prohibitive computational costs due to the exponentially growing search space.

2.2 Decomposition-Based Generalization

Apart from directly generalizing the model trained on a small-scale dataset to the large-scale instances, another line of research focuses on decomposing the large node graph into several small-scale subproblems. This approach involves solving them separately with a particular solver and then combining their solutions to form the solution of the large-scale problem [45–47, 12, 13, 48]. In particular, the problem decomposition and subproblem solving are often involved in different models. The task of the subproblem solver can be constructing a complete solution of a small-scale VRP or partial solutions of large-scale instances [16–18]. However, such decomposition introduces two critical shortcomings. When solving other complicated VRPs (e.g., CVRP), such decomposition becomes intractable and cannot be achieved by an individual strategy or model. Furthermore, when the decomposed subproblem is not small enough, it may still require other generalization techniques to solve.

2.3 Local Policy-Based Generalization

Another approach to solving large-scale VRPs is to reduce the search space to the K-Nearest-Neighbors (KNN) from the last visited node. The final decision is guided by either the original neural model with auxiliary distance information [49] or a local policy [14]. In addition, [15, 50, 42] directly select the candidate node from the neighborhood using NCO models. Although local policy can efficiently reduce the search space for constructive NCO, the reduced subgraph often drastically differs from the training instances, especially in large-scale or non-uniform instances. Consequently, the NCO models fail to distinguish the promising node. To this end, [15, 13, 19] propose a projection strategy to transform the extracted subgraph to a uniform distribution. While these strategies can enhance generalization, their effectiveness typically requires integration into model training, thereby imposing additional computational overhead and limiting their adaptability.

3 Preliminaries

VRP Definition The VRP is defined on a graph $G = (V, E)$, where $V = \{v_0, v_1, ..., v_n\}$ represents nodes (with v_0 as the depot in CVRP) and E denotes edges. Each non-depot node $V \backslash \{v_0\}$ has coordinates $s_i \in \mathbb{R}^2$ and a demand d_i, while v_0 has no demand. For the TSP, the objective is to find a single tour that explicitly visits all nodes once, minimizing the total Euclidean distance. In CVRP, vehicles with fixed capacity must deliver goods from the depot to customers, forming multiple routes that start and end at v_0. Each customer is visited once, and the cumulative demand per route cannot exceed the vehicle capacity. Solutions for both problems aim to minimize the total length of the tour, with feasibility requiring adherence to node visitation and capacity constraints.

Automatic Heuristic Design (AHD) AHD aims to automatically discover high-performing heuristics h for a target task T, such as combinatorial optimization. Formally, given a task T with input space X_T, AHD seeks to identify an optimal heuristic h^* from a heuristic space H by maximizing the expected performance over instances $x \in X_T$:

$$h^* = \arg\max_{h \in H} \mathbb{E}_{x \sim X_T} f_T(x, h), \tag{1}$$

where $f_T(x, h)$ quantifies the effectiveness of heuristic h on instance x. The heuristic space H encompasses all feasible strategies that adhere to the constraints of T. This approach aligns with hyper-heuristic methodologies [51], which automate heuristic selection or generation without domain-specific handcrafting.

LLM-Based AHD LLM-based AHD integrates LLMs into the evolutionary search for a high-performance heuristic [52–55]. This paradigm leverages LLMs to generate and refine heuristics through natural language reasoning and code synthesis. Within an evolutionary computation framework, LLMs simulate mutation and crossover operations by modifying or combining existing heuristics. For example, given a parent heuristic, LLMs can introduce new algorithmic components, adjust parameters, or merge features from multiple candidates, guided by linguistic prompts that encode task-specific objectives and constraints. This iterative process balances the exploration of high-quality candidates, enabling efficient traversal of the heuristic space H.

4 Distribution Projection in Large-Scale VRPs
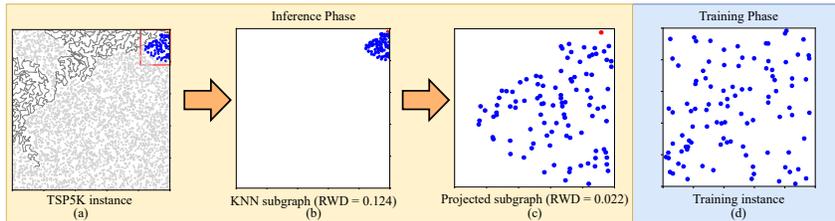
Figure 1: (a) Solution construction process for solving TSP5K instance, gray node, blue node, red node, and grey line denote the unvisited nodes, KNN (k=100) of the current node, current node, and constructed partial route, respectively. (b) Extracted KNN graph, RWD [56] indicates the distance between the input graph and a uniformly distributed training instance. (c) Projected KNN graph. (d) Training instance with 100 nodes.

When solving large-scale VRPs, current methods are facing challenges from the exponentially growing search space. As shown in the Figure. 1 (a), existing works reduce the search space to the KNN of the last visited node. Despite this reduction providing sufficient improvement, Figure. 1 (b) demonstrates that the selected KNN subgraphs come with various distributions that drastically differ from the training instance. Making it difficult for the model to predict the next promising node. Recent studies provide several projection techniques to project the input subgraph to a uniform distribution [15, 13, 19]. In this section, we systematically analyze the effectiveness of these projection methods and observe that such a technique has a great impact on the model's final performance.

Table 1: The effect of projection strategy on the gap in the LEHD model

Method	TSP1K Gap	TSP5K Gap	TSP10K Gap	TSP50K Gap	TSP100K Gap
LEHD w/o proj	4.45%	12.80%	17.42%	48.00%	121.42%
LEHD w/ proj	**2.96%**	**3.32%**	**3.77%**	**3.42%**	**3.24%**

To validate the effectiveness of the projection, we employ the LEHD [18] as the base model, restricting its search space to the KNN ($k = 100$) nodes from the last visited node. Then, we apply the projection method used in INViT [15] to map the subgraph. Subsequently, the LEHD is adopted to select one promising node within the transformed subgraph. The experimental results are provided in Table 1. The experiment results exhibit that LEHD with the INViT projection method outperforms LEHD without projection consistently on all scales in TSP.

These findings underscore the criticality of maintaining distribution consistency between the model's training data and its inference inputs for effective large-scale generalization. Projection techniques serve as a primary mechanism to achieve this alignment by transforming varied input distributions to the training set. Consequently, the development of more sophisticated and robust projections is crucial for advancing model generalization capabilities.
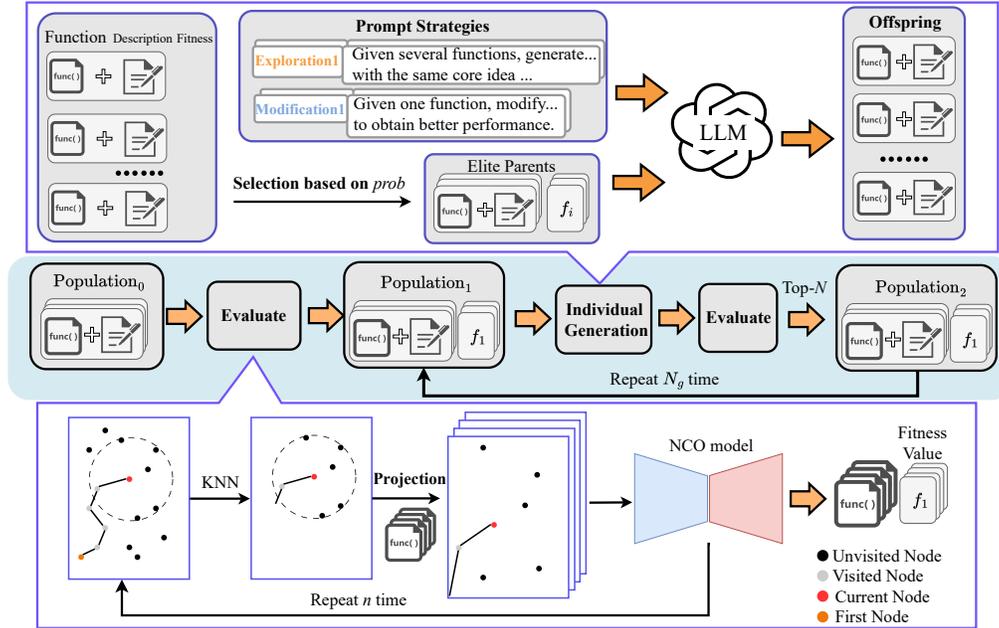
Figure 2: **The pipeline of the TTPL framework**. It comprises four components: initialization, fitness evaluation, offspring generation, and population update. **(a) Initialization:** TTPL establishes the initial population by generating individuals through prompting LLM with a predefined template. Following the initialization, an iterative optimization procedure is employed to search for the optimal individual. **(b) Offspring generation:** Offspring individuals are produced using several LLM-based evolutionary prompt strategies. **(c) Fitness evaluation:** An NCO model assesses the performance of these newly generated individuals. **(d) Population update:** The highest-performing individuals are then selected to constitute the succeeding generation, and this iterative process repeats until the specified termination criteria are satisfied.

5 Methodology

5.1 Test-Time Projection Learning

Current methods typically train models on small-scale, uniformly distributed datasets. However, these models often underperform on large-scale or real-world data due to the distributional shift between training and test instances. To address this challenge, we propose Test-Time Projection Learning (TTPL), an LLM-driven evolutionary framework that leverages LLM to generate an optimal projection strategy. Specifically, it comprises two components: 1) a NCO-based strategy evaluator is designed to measure the strategy generated by LLM; 2) an evolutionary projection strategy generator employs diverse prompt strategies to guide the LLM in developing these strategies.

Method Framework The overall framework of TTPL is demonstrated in the Algorithm. 1. Its inputs consist of the population size N, number of generations N_g, the NCO model f_θ, the LLM used to evolve the strategy, and the evaluation data set D. TTPL follows the general framework of EoH [52]. Therefore, we first generate N individuals using LLM with the prompts from EoH. Here, individuals consist of a description in natural language and a code block that implements the projection. These individuals are then evaluated by the NCO model f_θ to construct the initial population P_0. Moreover, we conduct N_g iterations to obtain an optimal projection strategy. In each iteration, we prompt LLMs to design different individuals based on a set of selected parents. Once the new population is generated, we select the first N best individuals as the next generation. Finally, it outputs the optimal strategy it found in previous iterations

---

Algorithm 1 $a^* = \textbf{TTPL}(N, N_g, f_\theta, \text{LLM}, D)$

1: **Input:**
2:     Population size: N; Number of Generation: N_g; NCO model: f_θ;
3:     A given LLM; Evaluation dataset D
4: **Output**:
5:     Code for the best found projection strategy: a^*
6: **Initialization:**
7: **for** $j = 1 : N$ **do**
8:     Initialize new individual a_j of the target model using LLM
9:     Evaluate a_j and obtain the fitness value $f_\theta(a_j)$ with evaluation dataset D
10: **end for**
11:     Construct initial population $P_0 = \{a_1, \ldots, a_N\}$
12: **for** $i = 1 : N_g$ **do**
13:     **for** $j = 1 : \text{N}$ **do**
14:         Generate new offspring using prompt strategies from [52]
15:         Evaluate offspring and obtain their fitness value with evaluation dataset D
16:     **end for**
17:     Construct offspring population O
18:     Sort O in descending order based on their fitness value
19:     Update P_{i-1} with the first N individuals in O
20: **end for**
21: **Return:** The best found projection strategy: a^*;

Individual Evaluation   To evaluate the LLM-designed strategies, we deploy them within the target NCO model and calculate the objective value on the evaluation dataset D. Specifically, given a current node v_i, we first select k nearest neighbors to form the subgraph G_k. Then, the strategy is performed on G_k to obtain the projected graph G_N. Moreover, we input the projected subgraph to the given NCO model f_θ and select a node within G_N as the destination of the next step. By repeating the above process, the final solution of a VRP instance is constructed step by step. Finally, the solution length is recorded as the fitness value of the input strategy.

Individual Generation   After initialization, N_g iterations are conducted to evolve the population. In each iteration, we first randomly select a set of parent individuals from the current population based on the probability:

$$prob_i = \frac{1/2^{r_i}}{\sum_{j=1}^{N} 1/2^{r_j}}, \tag{2}$$

where r_i is the rank of their fitness. After that, the selected parents are used to generate offspring through the four prompt strategies in [52], which consist of two groups, namely, Exploration (E1, E2) and Modification (M1, M2). The exploration prompt focuses on generating new individuals based on several selected parent strategies, while the modification prompt aims to modify the selected strategy for better performance. The details of four prompt strategies can be found in the Appendix. B.1

5.2   Multi-View Decision Fusion

Projection strategies transform the entire subgraph by a series of operations (e.g., rotation and translation) to align complex input distributions with the uniformly distributed training data. However, these graph-wise operations often struggle in normalizing local regions with density variations (i.e., strip-like node clusters in TSP), thereby impairing the model to distinguish promising nodes in local regions.

To resolve this limitation, we propose Multi-View Decision Fusion (MVDF), applied to the projected subgraphs. MVDF facilitates robust node identifications by generating multiple perspectives (views) of the subgraph. The model evaluates each perspective, and the resulting selection probabilities are aggregated. Ultimately, the perspective yielding the highest prediction score primarily guides the final decision.

In particular, given a subgraph with coordinates $\mathbf{X} \in \mathbb{R}^{k \times 2}$, we generate M augmented variants through geometric transformations $\mathcal{T}_m(\mathbf{X})$ proposed in [6]. Each augmented subgraph $\mathbf{X}_m = \mathcal{T}_m(\mathbf{X})$

is solved by the NCO model to produce logits $\mathbf{l}_m \in \mathbb{R}^K$. The final selection probability is derived by aggregating logits across all augmentations:

$$\mathbf{p} = \sigma\left(\sum_{m=1}^{M} \mathbf{l}_m\right), \tag{3}$$

where $\sigma\left(\cdot\right)$ denotes the softmax function. This ensemble strategy forces the model to learn transformation-invariant features, effectively neutralizing local density deviations.

6 Experiment

Table 2: Comparison results on the synthetic TSP and CVRP dataset. *: Results are directly cited from the original publications. N/A: results that exceed the time limitation (seven days). OOM: results that exceed GPU memory limits.

Method	TSP1K Obj.(Gap)	Time	TSP5K Obj.(Gap)	Time	TSP10K Obj.(Gap)	Time	TSP50K Obj.(Gap)	Time	TSP100K Obj.(Gap)	Time
LKH3	23.12 (0.00%)	1.7m	50.97 (0.00%)	12m	71.78 (0.00%)	33m	159.93 (0.00%)	10h	225.99 (0.00%)	25h
Concorde	23.12 (0.00%)	1m	50.95 (-0.05%)	31m	72.00 (0.15%)	1.4h	N/A	N/A	N/A	N/A
Random Insertion	26.11 (12.9%)	<1s	58.06 (13.9%)	<1s	81.82 (13.9%)	<1s	182.65 (14.2%)	15.4s	258.13 (14.2%)	1.7m
DIFUSCO*	23.39 (1.17%)	11.5s	——		73.62 (2.58%)	3.0m	——		——	
H-TSP	24.66 (6.66%)	48s	55.16 (8.21%)	1.2m	77.75 (8.38%)	2.2m	OOM		OOM	
GLOP	23.78 (2.85%)	10.2s	53.15 (4.26%)	1.0m	75.04 (4.39%)	1.9m	168.09 (5.10%)	1.5m	237.61 (5.14%)	3.9m
POMO aug * 8	32.51 (40.6%)	4.1s	87.72 (72.1%)	8.6m	OOM		OOM		OOM	
ELG aug * 8	25.738 (11.33%)	0.8s	60.19 (18.08%)	21s	OOM		OOM		OOM	
LEHD RRC1,000	23.29 (0.72%)	3.3m	54.43 (6.79%)	8.6m	80.90 (12.5%)	18.6m	OOM		OOM	
BQ bs16	23.43 (1.37%)	13s	58.27 (10.7%)	24s	OOM		OOM		OOM	
SIGD bs16	23.36 (1.03%)	17.3s	55.77 (9.42%)	30.5m	OOM		OOM		OOM	
INViT-3V greedy	24.66 (6.90%)	9.0s	54.49 (6.90%)	1.2m	76.85 (7.07%)	3.7m	171.42 (7.18%)	1.3h	242.26 (7.20%)	5.0h
LEHD greedy	23.84 (3.11%)	0.8s	58.85 (15.46%)	1.5m	91.33 (27.24%)	11.7m	OOM		OOM	
BQ greedy	23.65 (2.30%)	0.9s	58.27 (14.31%)	22.5s	89.73 (25.02%)	1.0m	OOM		OOM	
SIGD greedy	23.573 (1.96%)	1.2s	57.19 (12.20%)	15.5m	93.80 (30.68%)	15.5m	OOM		OOM	
TTPL	23.73 (2.65%)	0.1s	52.63 (3.25%)	1.4s	74.39 (3.63%)	2.9s	165.19 (3.29%)	14.3s	233.26 (3.22%)	28.9s
TTPL-MVDF	23.64 (2.26%)	0.5s	52.43 (2.86%)	3.2s	73.49 (2.39%)	7.2s	164.24 (2.69%)	32.1s	231.78 (2.56%)	1.1m
TTPL-MVDF RRC1000	**23.19 (0.28%)**	3.6m	**51.50 (1.04%)**	4.9m	**72.59 (1.13%)**	5.0m	**162.40 (1.55%)**	5.4m	**229.66 (1.63%)**	5.9m

Method	CVRP1K Obj.(Gap)	Time	CVRP5K Obj.(Gap)	Time	CVRP10K Obj.(Gap)	Time	CVRP50K Obj.(Gap)	Time	CVRP100K Obj.(Gap)	Time
HGS	41.2 (0.00%)	5m	126.2 (0.00%)	5m	227.3 (0.00)	5m	1081.0 (0.00%)	4h	2087.5 (0.00%)	6.3h
GLOP-G (LKH-3)	45.9 (11.4%)	1.1s	140.6 (11.4%)	4.0s	256.4 (11.1%)	6.2s	OOM		OOM	
POMO aug * 8	101 (145.15%)	4.6s	632.9 (401.51%)	11m	OOM		OOM		OOM	
ELG aug * 8	46.4 (12.62%)	10.3s	OOM		OOM		OOM		OOM	
LEHD RRC1,000	**42.4 (2.91%)**	3.4m	132.7 (5.15%)	10m	243.8 (7.28%)	51.6m	OOM		OOM	
BQ bs16	43.1 (4.61%)	14s	136.4 (8.08%)	2.4m	OOM		OOM		OOM	
SIGD bs16	44.3 (7.54%)	22.5s	137.5 (9.15%)	2.7m	247.2 (9.01%)	6.0m	1255.5 (16.30%)	39.3m	OOM	
INViT-3V greedy	48.2 (16.99%)	11s	146.6 (16.16%)	1.4m	262.1 (15.31%)	4.3m	1331.1 (23.1%)	1.5h	2683.4 (28.55%)	5.8h
LEHD greedy	44 (6.80%)	0.8s	138.2 (9.51%)	1.4m	256.3 (12.76%)	12m	OOM		OOM	
BQ greedy	44.2 (7.28%)	1s	139.9 (10.86%)	18.5s	262.2 (15.35%)	2m	OOM		OOM	
SIGD greedy	45.4 (10.39%)	4.5s	140.2 (11.31%)	9.1s	252.5 (11.34%)	48.9s	1274.3 (18.02%)	10.2m	OOM	
TTPL	44.7 (8.60%)	0.1s	134.4 (6.44%)	0.5s	238.9 (5.11%)	3.8s	1143.2 (5.72%)	19.4s	2220.4 (6.33%)	41.3s
TTPL-MVDF	44.4 (7.79%)	0.5s	132.4 (4.88%)	2.5s	233.0 (2.54%)	7.7s	1110.9 (2.73%)	40.5s	2163.5 (3.60%)	1.3m
TTPL-MVDF RRC1000	42.5 (3.28%)	4.1m	**129.2 (2.37%)**	4.0m	**229.6 (1.02%)**	6.4m	**1105.6 (2.25%)**	7.0m	**2157.5 (3.32%)**	7.7m

Problem Setting We evaluate our method on TSP and CVRP instances. Following established benchmarks [47, 18], the test sets include 128 instances for TSP1K and 16 instances each for TSP5K, 10K, 50K, and 100K. For CVRP, we use 100 instances for CVRP1K and CVRP5K and 16 instances each for CVRP10K, CVRP50K, and CVRP100K. CVRP capacities are 200 for CVRP1K and 300 for CVRP5K/10K/50K/100K. Optimal TSP solutions are calculated using LKH3 [57], while CVRP solutions are derived using HGS [58]. To further assess generalization, we follow [44] and evaluate on real-world instances from TSPLIB [59] and CVRPLIB [60], selecting symmetric EUC_2D instances with over 1K nodes (33 TSP and 14 CVRP instances). This ensures alignment with both synthetic benchmarks and practical scenarios.

Model Setting Our experiments adopt LEHD as the base model [18], aligning with its original architecture and hyperparameters. The embedding dimension is configured to 128, and the decoder comprises 6 attention layers. Each multi-head attention layer uses 8 heads, while the feed-forward layer dimension is set to 512. We configure the KNN to 100. All experiments are performed on a single NVIDIA GeForce RTX 3090 GPU with 24GB of memory.

LLM-AHD Setting The evolutionary framework follows the approach proposed by EoH [52]. The population size is set to 20, and the evolution process is run for 105 generations. The parent heuristic

is set to 2. The GPT-4o-mini model serves as the LLM backbone. For TSP/CVRP 1K, 5K, and 10K, we optimize one projection strategy for each scale, and generalize the strategy optimized on 10K to TSP/CVRP 50K and 100K due to the computational burden. At the beginning of the optimization, we input the projection strategy proposed in [15] as a seed to guide the heuristic design.

Baselines We compare TTPL with six categories of methods: **Classical Solvers:** Concorde [61], LKH3 [57] and HGS [58]; **Insertion Heuristic:** Random Insertion; **Construction-based NCO Methods:** POMO [7], BQ [42], LEHD [18], INVIT [15] and SIGD [62]; **Heatmap-based Methods:** DIFUSCO [28]; **Decomposition-based Method:** GLOP [13], H-TSP [12]; **Local Construction-based Method:** ELG [14].

Metrics and Inference We evaluate the performance using the optimality gap and inference time. The optimality gap quantifies the percentage difference between solutions generated by our method and the ground truth obtained from LKH3 (TSP) or HGS (CVRP). Inference time, reported in seconds (s), minutes (m), and hours (h), captures the computational efficiency of generating solutions across varying problem scales. For TTPL, we report three types of results, those obtained by greedy trajectory with a purely designed projection method, those obtained by greedy trajectory with our designed projection and MVDF, and those obtained with projection, MVDF, and Random Re-Construction (RRC) under 1000 iterations [18].

6.1 Experimental Results

Results on Synthetic Dataset Table 2 presents the comparative results, underscoring our method's superior performance and robust generalization capabilities across various problem scales. For TSP instances, our method, when relying on purely greedy construction, outperforms other greedy constructive methods on most problem scales, except TSP1K. However, by incorporating RRC for 1000 iterations, our approach consistently delivers the best performance across all TSP scales. Specifically, it reduces the optimality gap by 61.11%, 75.59%, 56.2%, 69.61%, and 68.29% for the TSP1K, 5K, 10K, 50K, and 100K instances, respectively, when compared to the leading alternative method. In the context of CVRP, our method, utilizing purely greedy sampling, secures the best results on all scales, with the exception of CVRP1K. Furthermore, by integrating RRC, our method is able to significantly surpass all other approaches across all evaluated CVRP scales. This translates to optimality gap reductions of 53.98%, 85.99%, 86.20%, and 88.37% on CVRP5K, 10K, 50K, and 100K instances, respectively, relative to the strongest competing baseline methods.

Table 3: Result on TSPLIB and CVRPLIB. OOM: results that exceed GPU memory limits. †: several instances are not solvable due to exceeding GPU memory limits.

Method	TSPLIB				CVRPLIB			
	1K < n ≤ 5K	n > 5K	All	Solved #	1K < n ≤ 7K	n > 7K	All	Solved #
GLOP	5.02%	6.87% †	5.50%	31/33	15.34%	21.32%	17.90%	14/14
ELG aug×8	11.34%	OOM	11.34%	23/33	10.57%	OOM	10.57%	6/14
BQ bs16	10.65%	30.58% †	12.95%	26/33	13.92%	OOM	13.92%	8/14
LEHD RRC1,000	4.00%	18.46% †	7.37%	30/33	8.42%	21.53% †	11.04%	10/14
SIGD greedy	12.37%	152.88% †	48.63%	31/33	14.73%	49.49%	29.63%	14/14
BQ greedy	11.64%	162.12% †	64.65%	32/33	16.92%	52.27%	32.07%	14/14
INViT greedy	11.49%	10.00%	11.04%	33/33	15.87%	26.64%	20.49%	14/14
LEHD greedy	11.14%	39.34% †	17.72%	30/33	15.20%	32.80% †	18.72%	10/14
TTPL	6.04%	4.57%	5.80%	33/33	11.89%	14.93%	13.19%	14/14
TTPL-MVDF	3.81%	4.05%	3.88%	33/33	10.41%	11.71%	10.97%	14/14
TTPL-MVDF RRC1000	**1.04%**	**2.12%**	**1.37%**	33/33	**5.20%**	**10.56%**	**7.50%**	14/14

Results on Benchmark We further test our method on TSPLIB [59] and CVRPLIB [60]. The detailed results are demonstrated in the Table 3. When using greedy construction for inference, LEHD purely with our designed projection can achieve a better result than other construction-based methods on all groups of instances. Using the MVDF and RRC further strengthens our performance, which yields a significant gap between the second-best methods.

6.2 Ablation Study

8

Table 4: Comparison between different projection strategies on the synthetic TSP dataset.

| | TSP1K | | TSP5K | | TSP10K | | TSP50K | | TSP100K | |
	Obj.(Gap)	Time	Obj.(Gap)	Time	Obj.(Gap)	Time	Obj.(Gap)	Time	Obj.(Gap)	Time
w/o proj	24.2 (4.49%)	0.1s	57.5 (12.80%)	1.4s	84.3 (17.42%)	2.7s	236.7 (48.00%)	13.2s	500.4 (121.42%)	27.8s
seed proj	23.8 (2.96%)	0.1s	52.7 (3.32%)	1.5s	74.5 (3.77%)	2.9s	165.4 (3.42%)	14.4s	233.3 (3.24%)	29.6s
TTPL	**23.73 (2.65%)**	0.1s	**52.63 (3.25%)**	1.4s	**74.39 (3.63%)**	2.9s	**165.19 (3.29%))**	14.3s	**233.26 (3.22%)**	28.9s

Effects of Designed Projection   To validate the effectiveness of the LLM-designed projection strategy, we design two variants of our method: 1) w/o proj: LEHD only uses KNN to reduce the search space during inference. 2) seed proj: The projection strategy is replaced with the input seed strategy in [15]. As exhibited in the Table. 4, the projection strategy designed from the TTPL framework consistently outperforms the two variants on all scales.

Table 5: Comparison between LEHD with MVDF, POMO aug, and without MVDF on synthetic TSP dataset

| | TSP1K | | TSP5K | | TSP10K | | TSP50K | | TSP100K | |
	Obj.(Gap)	Time	Obj.(Gap)	Time	Obj.(Gap)	Time	Obj.(Gap)	Time	Obj.(Gap)	Time
w/o MVDF	23.7 (2.65%)	0.1s	52.6 (3.25%)	1.4s	74.4 (3.63%)	2.9s	165.2 (3.29%)	14.3s	233.3 (3.22%)	28.9s
POMO aug	**23.4 (0.89%)**	0.5s	**52.1 (2.22%)**	3.1s	73.6 (2.56%)	6.3s	164.5 (2.86%)	36.6s	232.4 (2.85%)	1.5m
TTPL-MVDF	23.6 (2.26%)	0.5s	52.4 (2.86%)	3.2s	**73.5 (2.39%)**	7.2s	**164.2 (2.69%)**	32.1s	**231.8 (2.56%)**	1.1m

Effects of MVDF   To assess the efficacy of our proposed MVDF, we compare our complete method against two configurations: 1) w/o MVDF: LEHD utilizes the designed projection but without MVDF during inference; 2) POMO aug: test instances are first augmented using the POMO augmentation [7], and then solved with LEHD equipped with the designed projection. The complete results are shown in Table 5. Our MVDF approach outperforms the w/o MVDF variant in 5 out of 5 cases and the POMO aug variant in 3 out of 5 cases. Notably, MVDF demonstrates particular effectiveness when solving large-scale instances.

6.3   Versatility study

Table 6: Results of TTPL-MVDF designed strategy performed on POMO on randomly generated test instances

| | TSP1K | | TSP5K | | TSP10K | | TSP50K | | TSP100K | |
	Obj.	Time	Obj.	Time	Obj.	Time	Obj.	Time	Obj.	Time
POMO knn	33.4	0.2s	96.1	3.8s	153.4	7.5s	392.4	38.5s	597.8	1.3m
POMO seed	30.0	0.2s	73.8	4.0s	103.0	7.9s	235.8	39.9s	331.3	1.3m
POMO Ours	**29.8**	1.3s	**67.6**	7.8s	**94.6**	15.5s	**212.1**	1.3m	**296.6**	2.6m

Versatility on the Other Model   The versatility of our proposed techniques is further investigated by replacing the base model from LEHD with POMO, a well-known model trained by RL. We compare POMO, which is equipped with our proposed projection and MVDF technique, against POMO using KNN and the seed projection method. As shown in the Table 6, our method on POMO surpasses the compared approaches, indicating promising adaptability to different base models.

Versatility on Different Distributions   The robustness of TTPL-MVDF is evaluated on cross-distribution instances (cluster, explosion, and implosion) from [15]. Compared against LEHD without projection and LEHD with seed projection, TTPL-MVDF demonstrates a significant improvement in the base model's robustness. These findings (see Appendix D.2 for full results) validate the effectiveness of our proposed method in handling distributional shifts.

7   Conclusion, Limitation, and Future Work

In this work, we have presented an LLM-driven projection learning framework to improve model generalization in large-scale vehicle routing problems (VRPs). The core idea is to utilize an LLM to model the relationship between training and test data distribution, thereby informing the generation of an optimized projection strategy. To further boost performance, we have developed Multi-View

Decision Fusion (MVDF), which presents the model with multiple views of the original problem instance, enabling it to select the most confident one to guide node selection at each construction step. Empirical evaluation on diverse synthetic and real-world TSP and CVRP benchmarks confirms that our approach markedly enhances the zero-shot generalization capability of a base model (trained solely on 100-node instances) to large-scale instances.

Limitation and Future Work While TTPL-MVDF shows superior performance on large-scale instances, a limitation of TTPL-MVDF is the relatively slow convergence to optimal strategies within its LLM optimization phase. In the future, we will investigate more efficient LLM optimization operators for improved evolution speed.

Acknowledgments and Disclosure of Funding

References

[1] Matthew Veres and Medhat Moussa. Deep learning for intelligent transportation systems: A survey of emerging trends. *IEEE Transactions on Intelligent Transportation Systems*, 21(8):3152–3168, 2019.

[2] Alexandre Laterre, Yunguan Fu, Mohamed Khalil Jabri, Alain-Sam Cohen, David Kas, Karl Hajjar, Torbjorn S Dahl, Amine Kerkeni, and Karim Beguir. Ranked reward: Enabling self-play reinforcement learning for combinatorial optimization. *arXiv preprint arXiv:1807.01672*, 2018.

[3] Antonio Giallanza and Gabriella Li Puma. Fuzzy green vehicle routing problem for designing a three echelons supply chain. *Journal of Cleaner Production*, 259:120774, 2020.

[4] Giorgio Ausiello, Pierluigi Crescenzi, Giorgio Gambosi, Viggo Kann, Alberto Marchetti-Spaccamela, and Marco Protasi. *Complexity and approximation: Combinatorial optimization problems and their approximability properties*. Springer Science & Business Media, 2012.

[5] Yoshua Bengio, Andrea Lodi, and Antoine Prouvost. Machine learning for combinatorial optimization: a methodological tour d'horizon. *European Journal of Operational Research*, 290(2):405–421, 2021.

[6] Wouter Kool, Herke Van Hoof, and Max Welling. Attention, learn to solve routing problems! *arXiv preprint arXiv:1803.08475*, 2018.

[7] Yeong-Dae Kwon, Jinho Choo, Byoungjip Kim, Iljoo Yoon, Youngjune Gwon, and Seungjai Min. Pomo: Policy optimization with multiple optima for reinforcement learning. *Advances in Neural Information Processing Systems*, 33:21188–21198, 2020.

[8] André Hottung, Yeong-Dae Kwon, and Kevin Tierney. Efficient active search for combinatorial optimization problems. *arXiv preprint arXiv:2106.05126*, 2021.

[9] Changliang Zhou, Canhong Yu, Shunyu Yao, Xi Lin, Zhenkun Wang, Yu Zhou, and Qingfu Zhang. Urs: A unified neural routing solver for cross-problem zero-shot generalization. *arXiv preprint arXiv:2509.23413*, 2025.

[10] Yan Jin, Yuandong Ding, Xuanhao Pan, Kun He, Li Zhao, Tao Qin, Lei Song, and Jiang Bian. Pointerformer: Deep reinforced multi-pointer transformer for the traveling salesman problem. In *Proceedings of the AAAI Conference on Artificial Intelligence*, volume 37, pages 8132–8140, 2023.

[11] Jianan Zhou, Yaoxin Wu, Wen Song, Zhiguang Cao, and Jie Zhang. Towards omni-generalizable neural methods for vehicle routing problems. In *International Conference on Machine Learning*, pages 42769–42789. PMLR, 2023.

[12] Xuanhao Pan, Yan Jin, Yuandong Ding, Mingxiao Feng, Li Zhao, Lei Song, and Jiang Bian. H-tsp: Hierarchically solving the large-scale traveling salesman problem. In *Proceedings of the AAAI Conference on Artificial Intelligence*, volume 37, pages 9345–9353, 2023.

[13] Haoran Ye, Jiarui Wang, Helan Liang, Zhiguang Cao, Yong Li, and Fanzhang Li. Glop: Learning global partition and local construction for solving large-scale routing problems in real-time. In *Proceedings of the AAAI Conference on Artificial Intelligence*, volume 38, pages 20284–20292, 2024.

[14] Chengrui Gao, Haopu Shang, Ke Xue, Dong Li, and Chao Qian. Towards generalizable neural solvers for vehicle routing problems via ensemble with transferrable local policy. *arXiv preprint arXiv:2308.14104*, 2023.

[15] Han Fang, Zhihao Song, Paul Weng, and Yutong Ban. Invit: A generalizable routing problem solver with invariant nested view transformer. *arXiv preprint arXiv:2402.02317*, 2024.

[16] Minsu Kim, Jinkyoo Park, et al. Learning collaborative policies to solve np-hard routing problems. *Advances in Neural Information Processing Systems*, 34:10418–10430, 2021.

[17] Hanni Cheng, Haosi Zheng, Ya Cong, Weihao Jiang, and Shiliang Pu. Select and optimize: Learning to solve large-scale tsp instances. In *International Conference on Artificial Intelligence and Statistics*, pages 1219–1231. PMLR, 2023.

[18] Fu Luo, Xi Lin, Fei Liu, Qingfu Zhang, and Zhenkun Wang. Neural combinatorial optimization with heavy decoder: Toward large scale generalization. *Advances in Neural Information Processing Systems*, 36:8845–8864, 2023.

[19] Zhang-Hua Fu, Kai-Bin Qiu, and Hongyuan Zha. Generalize a small pre-trained model to arbitrarily large tsp instances. In *Proceedings of the AAAI conference on artificial intelligence*, volume 35, pages 7474–7482, 2021.

[20] Ziwei Huang, Jianan Zhou, Zhiguang Cao, and Yixin Xu. Rethinking light decoder-based solvers for vehicle routing problems. *arXiv preprint arXiv:2503.00753*, 2025.

[21] Yeong-Dae Kwon, Jinho Choo, Iljoo Yoon, Minah Park, Duwon Park, and Youngjune Gwon. Matrix encoding networks for neural combinatorial optimization. *Advances in Neural Information Processing Systems*, 34:5138–5149, 2021.

[22] Darko Drakulic, Sofia Michel, and Jean-Marc Andreoli. Goal: A generalist combinatorial optimization agent learner. In *The Thirteenth International Conference on Learning Representations*, 2024.

[23] Fei Liu, Xi Lin, Zhenkun Wang, Qingfu Zhang, Tong Xialiang, and Mingxuan Yuan. Multi-task learning for routing problem with cross-problem zero-shot generalization. In *Proceedings of the 30th ACM SIGKDD Conference on Knowledge Discovery and Data Mining*, pages 1898–1908, 2024.

[24] Jianan Zhou, Zhiguang Cao, Yaoxin Wu, Wen Song, Yining Ma, Jie Zhang, and Chi Xu. Mvmoe: Multi-task vehicle routing solver with mixture-of-experts. *arXiv preprint arXiv:2405.01029*, 2024.

[25] Elias Khalil, Hanjun Dai, Yuyu Zhang, Bistra Dilkina, and Le Song. Learning combinatorial optimization algorithms over graphs. *Advances in neural information processing systems*, 30, 2017.

[26] Ni Zhang, Jingfeng Yang, Zhiguang Cao, and Xu Chi. Adversarial generative flow network for solving vehicle routing problems. *arXiv preprint arXiv:2503.01931*, 2025.

[27] Yang Li, Jinpei Guo, Runzhong Wang, and Junchi Yan. T2t: From distribution learning in training to gradient search in testing for combinatorial optimization. *Advances in Neural Information Processing Systems*, 36:50020–50040, 2023.

[28] Zhiqing Sun and Yiming Yang. DIFUSCO: Graph-based diffusion solvers for combinatorial optimization. *Advances in neural information processing systems*, 36:3706–3731, 2023.

[29] Yang Li, Jinpei Guo, Runzhong Wang, Hongyuan Zha, and Junchi Yan. Fast t2t: Optimization consistency speeds up diffusion-based training-to-testing solving for combinatorial optimization. *Advances in Neural Information Processing Systems*, 37:30179–30206, 2024.

[30] Oriol Vinyals, Meire Fortunato, and Navdeep Jaitly. Pointer networks. *Advances in neural information processing systems*, 28, 2015.

[31] Irwan Bello, Hieu Pham, Quoc V Le, Mohammad Norouzi, and Samy Bengio. Neural combinatorial optimization with reinforcement learning. *arXiv preprint arXiv:1611.09940*, 2016.

[32] Mohammadreza Nazari, Afshin Oroojlooy, Lawrence Snyder, and Martin Takác. Reinforcement learning for solving the vehicle routing problem. *Advances in neural information processing systems*, 31, 2018.

[33] Michel Deudon, Pierre Cournut, Alexandre Lacoste, Yossiri Adulyasak, and Louis-Martin Rousseau. Learning heuristics for the tsp by policy gradient. In *Integration of Constraint Programming, Artificial Intelligence, and Operations Research: 15th International Conference, CPAIOR 2018, Delft, The Netherlands, June 26–29, 2018, Proceedings 15*, pages 170–181. Springer, 2018.

[34] Ashish Vaswani, Noam Shazeer, Niki Parmar, Jakob Uszkoreit, Llion Jones, Aidan N Gomez, Łukasz Kaiser, and Illia Polosukhin. Attention is all you need. *Advances in neural information processing systems*, 30, 2017.

[35] Liang Xin, Wen Song, Zhiguang Cao, and Jie Zhang. Step-wise deep learning models for solving routing problems. *IEEE Transactions on Industrial Informatics*, 17(7):4861–4871, 2020.

[36] Rui Sun, Zhi Zheng, and Zhenkun Wang. Learning encodings for constructive neural combinatorial optimization needs to regret. In *Proceedings of the AAAI Conference on Artificial Intelligence*, volume 38, pages 20803–20811, 2024.

[37] Zhi Zheng, Shunyu Yao, Zhenkun Wang, Tong Xialiang, Mingxuan Yuan, and Ke Tang. DPN: Decoupling partition and navigation for neural solvers of min-max vehicle routing problems. In *Forty-first International Conference on Machine Learning*, 2024. URL https://openreview.net/forum?id=ar174skI9u.

[38] Changliang Zhou, Xi Lin, Zhenkun Wang, Xialiang Tong, Mingxuan Yuan, and Qingfu Zhang. Instance-conditioned adaptation for large-scale generalization of neural combinatorial optimization. *arXiv preprint arXiv:2405.01906*, 2024.

[39] Zhi Zheng, Shunyu Yao, Genghui Li, Linxi Han, and Zhenkun Wang. Pareto improver: Learning improvement heuristics for multi-objective route planning. *IEEE Transactions on Intelligent Transportation Systems*, 25(1):1033–1043, 2024. doi: 10.1109/TITS.2023.3313688.

[40] Han Li, Fei Liu, Zhi Zheng, Yu Zhang, and Zhenkun Wang. CaDA: Cross-problem routing solver with constraint-aware dual-attention. In *International Conference on Machine Learning*, 2025. URL https://openreview.net/forum?id=CS4RyQuTig.

[41] Fu Luo, Yaoxin Wu, Zhi Zheng, and Zhenkun Wang. Rethinking neural combinatorial optimization for vehicle routing problems with different constraint tightness degrees, 2025. URL https://arxiv.org/abs/2505.24627.

[42] Darko Drakulic, Sofia Michel, Florian Mai, Arnaud Sors, and Jean-Marc Andreoli. Bq-nco: Bisimulation quotienting for efficient neural combinatorial optimization. *Advances in Neural Information Processing Systems*, 36:77416–77429, 2023.

[43] Yuhong Cao, Zhanhong Sun, and Guillaume Sartoretti. Dan: Decentralized attention-based neural network for the minmax multiple traveling salesman problem. In *International Symposium on Distributed Autonomous Robotic Systems*, pages 202–215. Springer, 2022.

[44] Fu Luo, Xi Lin, Yaoxin Wu, Zhenkun Wang, Tong Xialiang, Mingxuan Yuan, and Qingfu Zhang. Boosting neural combinatorial optimization for large-scale vehicle routing problems. In *International Conference on Learning Representations*, 2025.

[45] Sirui Li, Zhongxia Yan, and Cathy Wu. Learning to delegate for large-scale vehicle routing. *Advances in Neural Information Processing Systems*, 34:26198–26211, 2021.

[46] Zefang Zong, Hansen Wang, Jingwei Wang, Meng Zheng, and Yong Li. Rbg: Hierarchically solving large-scale routing problems in logistic systems via reinforcement learning. In *Proceedings of the 28th ACM SIGKDD Conference on Knowledge Discovery and Data Mining*, pages 4648–4658, 2022.

[47] Qingchun Hou, Jingwei Yang, Yiqiang Su, Xiaoqing Wang, and Yuming Deng. Generalize learned heuristics to solve large-scale vehicle routing problems in real-time. In *International Conference on Learning Representations*, 2023.

[48] Zhi Zheng, Changliang Zhou, Tong Xialiang, Mingxuan Yuan, and Zhenkun Wang. UDC: A unified neural divide-and-conquer framework for large-scale combinatorial optimization problems. In *Advances in Neural Information Processing Systems*, 2024.

[49] Yang Wang, Ya-Hui Jia, Wei-Neng Chen, and Yi Mei. Distance-aware attention reshaping: Enhance generalization of neural solver for large-scale vehicle routing problems. *arXiv preprint arXiv:2401.06979*, 2024.

[50] Changliang Zhou, Xi Lin, Zhenkun Wang, and Qingfu Zhang. L2r: Learning to reduce search space for generalizable neural routing solver. *arXiv preprint arXiv:2503.03137*, 2025.

[51] Edmund K Burke, Michel Gendreau, Matthew Hyde, Graham Kendall, Gabriela Ochoa, Ender Özcan, and Rong Qu. Hyper-heuristics: A survey of the state of the art. *Journal of the Operational Research Society*, 64(12):1695–1724, 2013.

[52] Fei Liu, Xialiang Tong, Mingxuan Yuan, Xi Lin, Fu Luo, Zhenkun Wang, Zhichao Lu, and Qingfu Zhang. Evolution of heuristics: Towards efficient automatic algorithm design using large language mode.(2024). *arXiv preprint arXiv:2401.02051*, 2024.

[53] Zhi Zheng, Zhuoliang Xie, Zhenkun Wang, and Bryan Hooi. Monte carlo tree search for comprehensive exploration in LLM-based automatic heuristic design. In *International Conference on Machine Learning*, 2025. URL `https://openreview.net/forum?id=Do1OdZzYHr`.

[54] Kai Li, Fei Liu, Zhenkun Wang, Xialiang Tong, Xiongwei Han, Mingxuan Yuan, and Qingfu Zhang. Ars: Automatic routing solver with large language models. *arXiv preprint arXiv:2502.15359*, 2025.

[55] Kai Li, Ruihao Zheng, Xinye Hao, and Zhenkun Wang. Multi-objective infeasibility diagnosis for routing problems using large language models. *arXiv preprint arXiv:2508.03406*, 2025.

[56] Xu Wang, Fuyou Miao, Wenjie Liu, and Yan Xiong. Efficient and robust neural combinatorial optimization via wasserstein-based coresets. In *The Thirteenth International Conference on Learning Representations*.

[57] Keld Helsgaun. An extension of the lin-kernighan-helsgaun tsp solver for constrained traveling salesman and vehicle routing problems. *Roskilde: Roskilde University*, 12:966–980, 2017.

[58] Thibaut Vidal. Hybrid genetic search for the cvrp: Open-source implementation and swap* neighborhood. *Computers & Operations Research*, 140:105643, 2022.

[59] Gerhard Reinelt. Tsplib—a traveling salesman problem library. *ORSA journal on computing*, 3(4):376–384, 1991.

[60] Eduardo Uchoa, Diego Pecin, Artur Pessoa, Marcus Poggi, Thibaut Vidal, and Anand Subramanian. New benchmark instances for the capacitated vehicle routing problem. *European Journal of Operational Research*, 257(3):845–858, 2017.

[61] Robert Bixby Vašek Chvátal David Applegate and William Cook. Concorde tsp solver. Concorde tsp solver. 2006.

[62] Jonathan Pirnay and Dominik G Grimm. Self-improvement for neural combinatorial optimization: Sample without replacement, but improvement. *arXiv preprint arXiv:2403.15180*, 2024.

[63] Xinyun Chen and Yuandong Tian. Learning to perform local rewriting for combinatorial optimization. *Advances in neural information processing systems*, 32, 2019.

[64] Zhuwen Li, Qifeng Chen, and Vladlen Koltun. Combinatorial optimization with graph convolutional networks and guided tree search. *Advances in neural information processing systems*, 31, 2018.

[65] André Hottung, Bhanu Bhandari, and Kevin Tierney. Learning a latent search space for routing problems using variational autoencoders. In *International Conference on Learning Representations*, 2021.

[66] Chaitanya K Joshi, Thomas Laurent, and Xavier Bresson. An efficient graph convolutional network technique for the travelling salesman problem. *arXiv preprint arXiv:1906.01227*, 2019.

[67] Wouter Kool, Herke van Hoof, Joaquim Gromicho, and Max Welling. Deep policy dynamic programming for vehicle routing problems. In *International conference on integration of constraint programming, artificial intelligence, and operations research*, pages 190–213. Springer, 2022.

[68] Benjamin Hudson, Qingbiao Li, Matthew Malencia, and Amanda Prorok. Graph neural network guided local search for the traveling salesperson problem. *arXiv preprint arXiv:2110.05291*, 2021.

[69] Ruizhong Qiu, Zhiqing Sun, and Yiming Yang. Dimes: A differentiable meta solver for combinatorial optimization problems. *Advances in Neural Information Processing Systems*, 35:25531–25546, 2022.

[70] Yining Ma, Jingwen Li, Zhiguang Cao, Wen Song, Le Zhang, Zhenghua Chen, and Jing Tang. Learning to iteratively solve routing problems with dual-aspect collaborative transformer. *Advances in Neural Information Processing Systems*, 34:11096–11107, 2021.

[71] Paulo R d O Costa, Jason Rhuggenaath, Yingqian Zhang, and Alp Akcay. Learning 2-opt heuristics for the traveling salesman problem via deep reinforcement learning. In *Asian conference on machine learning*, pages 465–480. PMLR, 2020.

[72] Quentin Cappart, Thierry Moisan, Louis-Martin Rousseau, Isabeau Prémont-Schwarz, and Andre A Cire. Combining reinforcement learning and constraint programming for combinatorial optimization. In *Proceedings of the AAAI Conference on Artificial Intelligence*, volume 35, pages 3677–3687, 2021.

[73] André Hottung and Kevin Tierney. Neural large neighborhood search for the capacitated vehicle routing problem. In *ECAI 2020*, pages 443–450. IOS Press, 2020.

[74] Liang Xin, Wen Song, Zhiguang Cao, and Jie Zhang. Neurolkh: Combining deep learning model with lin-kernighan-helsgaun heuristic for solving the traveling salesman problem. *Advances in Neural Information Processing Systems*, 34:7472–7483, 2021.

[75] Jialin Song, Yisong Yue, Bistra Dilkina, et al. A general large neighborhood search framework for solving integer linear programs. *Advances in Neural Information Processing Systems*, 33:20012–20023, 2020.

[76] Thomas Barrett, William Clements, Jakob Foerster, and Alex Lvovsky. Exploratory combinatorial optimization with reinforcement learning. In *Proceedings of the AAAI conference on artificial intelligence*, volume 34, pages 3243–3250, 2020.

[77] Yaoxin Wu, Wen Song, Zhiguang Cao, Jie Zhang, and Andrew Lim. Learning improvement heuristics for solving routing problems. *IEEE Transactions on Neural Networks and learning systems*, 33(9):5057–5069, 2021.

[78] Gurobi Optimization. Inc.,"gurobi optimizer reference manual," 2015. 2014.

[79] Bernardino Romera-Paredes, Mohammadamin Barekatain, Alexander Novikov, Matej Balog, M Pawan Kumar, Emilien Dupont, Francisco JR Ruiz, Jordan S Ellenberg, Pengming Wang, Omar Fawzi, et al. Mathematical discoveries from program search with large language models. *Nature*, 625(7995):468–475, 2024.

[80] Haoran Ye, Jiarui Wang, Zhiguang Cao, Federico Berto, Chuanbo Hua, Haeyeon Kim, Jinkyoo Park, and Guojie Song. Reevo: Large language models as hyper-heuristics with reflective evolution. *Advances in neural information processing systems*, 37:43571–43608, 2024.

[81] Pham Vu Tuan Dat, Long Doan, and Huynh Thi Thanh Binh. Hsevo: Elevating automatic heuristic design with diversity-driven harmony search and genetic algorithm using llms. In *Proceedings of the AAAI Conference on Artificial Intelligence*, volume 39, pages 26931–26938, 2025.

[82] David Applegate, Ribert Bixby, Vasek Chvatal, and William Cook. Concorde tsp solver, 2006.

[83] Fei Liu, Rui Zhang, Zhuoliang Xie, Rui Sun, Kai Li, Xi Lin, Zhenkun Wang, Zhichao Lu, and Qingfu Zhang. LLM4AD: A platform for algorithm design with large language model. *arXiv preprint arXiv:2412.17287*, 2024.

NeurIPS Paper Checklist

1. **Claims**

   Question: Do the main claims made in the abstract and introduction accurately reflect the paper's contributions and scope?

   Answer: [Yes]

   Justification: Yes, we clearly claim our contribution and scope in the abstract and introduction. Our primary contribution is a powerful projection technique designed to enhance model generalization for large-scale Vehicle Routing Problems (VRPs). This research is situated within the field of neural combinatorial optimization.

   Guidelines:

   - The answer NA means that the abstract and introduction do not include the claims made in the paper.
   - The abstract and/or introduction should clearly state the claims made, including the contributions made in the paper and important assumptions and limitations. A No or NA answer to this question will not be perceived well by the reviewers.
   - The claims made should match theoretical and experimental results, and reflect how much the results can be expected to generalize to other settings.
   - It is fine to include aspirational goals as motivation as long as it is clear that these goals are not attained by the paper.

2. **Limitations**

   Question: Does the paper discuss the limitations of the work performed by the authors?

   Answer: [Yes]

   Justification: We discuss our limitation in Section.7.

   Guidelines:

   - The answer NA means that the paper has no limitation while the answer No means that the paper has limitations, but those are not discussed in the paper.
   - The authors are encouraged to create a separate "Limitations" section in their paper.
   - The paper should point out any strong assumptions and how robust the results are to violations of these assumptions (e.g., independence assumptions, noiseless settings, model well-specification, asymptotic approximations only holding locally). The authors should reflect on how these assumptions might be violated in practice and what the implications would be.
   - The authors should reflect on the scope of the claims made, e.g., if the approach was only tested on a few datasets or with a few runs. In general, empirical results often depend on implicit assumptions, which should be articulated.
   - The authors should reflect on the factors that influence the performance of the approach. For example, a facial recognition algorithm may perform poorly when image resolution is low or images are taken in low lighting. Or a speech-to-text system might not be used reliably to provide closed captions for online lectures because it fails to handle technical jargon.
   - The authors should discuss the computational efficiency of the proposed algorithms and how they scale with dataset size.
   - If applicable, the authors should discuss possible limitations of their approach to address problems of privacy and fairness.
   - While the authors might fear that complete honesty about limitations might be used by reviewers as grounds for rejection, a worse outcome might be that reviewers discover limitations that aren't acknowledged in the paper. The authors should use their best judgment and recognize that individual actions in favor of transparency play an important role in developing norms that preserve the integrity of the community. Reviewers will be specifically instructed to not penalize honesty concerning limitations.

3. **Theory assumptions and proofs**

   Question: For each theoretical result, does the paper provide the full set of assumptions and a complete (and correct) proof?

Answer: [NA]

Justification: This paper does not incorporate theoretical results; all results presented in this paper are experimental.

Guidelines:

- The answer NA means that the paper does not include theoretical results.
- All the theorems, formulas, and proofs in the paper should be numbered and cross-referenced.
- All assumptions should be clearly stated or referenced in the statement of any theorems.
- The proofs can either appear in the main paper or the supplemental material, but if they appear in the supplemental material, the authors are encouraged to provide a short proof sketch to provide intuition.
- Inversely, any informal proof provided in the core of the paper should be complemented by formal proofs provided in appendix or supplemental material.
- Theorems and Lemmas that the proof relies upon should be properly referenced.

4. **Experimental result reproducibility**

Question: Does the paper fully disclose all the information needed to reproduce the main experimental results of the paper to the extent that it affects the main claims and/or conclusions of the paper (regardless of whether the code and data are provided or not)?

Answer: [Yes]

Justification: We specify the details to reproduce our results in Section. 6. In particular, it contains the model architecture, dataset description, parameter settings, and experimental setups. All of them ensure our experiment results can be independently reproduced.

Guidelines:

- The answer NA means that the paper does not include experiments.
- If the paper includes experiments, a No answer to this question will not be perceived well by the reviewers: Making the paper reproducible is important, regardless of whether the code and data are provided or not.
- If the contribution is a dataset and/or model, the authors should describe the steps taken to make their results reproducible or verifiable.
- Depending on the contribution, reproducibility can be accomplished in various ways. For example, if the contribution is a novel architecture, describing the architecture fully might suffice, or if the contribution is a specific model and empirical evaluation, it may be necessary to either make it possible for others to replicate the model with the same dataset, or provide access to the model. In general. releasing code and data is often one good way to accomplish this, but reproducibility can also be provided via detailed instructions for how to replicate the results, access to a hosted model (e.g., in the case of a large language model), releasing of a model checkpoint, or other means that are appropriate to the research performed.
- While NeurIPS does not require releasing code, the conference does require all submissions to provide some reasonable avenue for reproducibility, which may depend on the nature of the contribution. For example
  (a) If the contribution is primarily a new algorithm, the paper should make it clear how to reproduce that algorithm.
  (b) If the contribution is primarily a new model architecture, the paper should describe the architecture clearly and fully.
  (c) If the contribution is a new model (e.g., a large language model), then there should either be a way to access this model for reproducing the results or a way to reproduce the model (e.g., with an open-source dataset or instructions for how to construct the dataset).
  (d) We recognize that reproducibility may be tricky in some cases, in which case authors are welcome to describe the particular way they provide for reproducibility. In the case of closed-source models, it may be that access to the model is limited in some way (e.g., to registered users), but it should be possible for other researchers to have some path to reproducing or verifying the results.

16

5. **Open access to data and code**

   Question: Does the paper provide open access to the data and code, with sufficient instructions to faithfully reproduce the main experimental results, as described in supplemental material?

   Answer: [No]

   Justification: We will release our code and data once the paper is accepted.

   Guidelines:

   - The answer NA means that paper does not include experiments requiring code.
   - Please see the NeurIPS code and data submission guidelines (`https://nips.cc/public/guides/CodeSubmissionPolicy`) for more details.
   - While we encourage the release of code and data, we understand that this might not be possible, so "No" is an acceptable answer. Papers cannot be rejected simply for not including code, unless this is central to the contribution (e.g., for a new open-source benchmark).
   - The instructions should contain the exact command and environment needed to run to reproduce the results. See the NeurIPS code and data submission guidelines (`https://nips.cc/public/guides/CodeSubmissionPolicy`) for more details.
   - The authors should provide instructions on data access and preparation, including how to access the raw data, preprocessed data, intermediate data, and generated data, etc.
   - The authors should provide scripts to reproduce all experimental results for the new proposed method and baselines. If only a subset of experiments are reproducible, they should state which ones are omitted from the script and why.
   - At submission time, to preserve anonymity, the authors should release anonymized versions (if applicable).
   - Providing as much information as possible in supplemental material (appended to the paper) is recommended, but including URLs to data and code is permitted.

6. **Experimental setting/details**

   Question: Does the paper specify all the training and test details (e.g., data splits, hyperparameters, how they were chosen, type of optimizer, etc.) necessary to understand the results?

   Answer: [Yes]

   Justification: We introduce all experimental details in Section. 6.

   Guidelines:

   - The answer NA means that the paper does not include experiments.
   - The experimental setting should be presented in the core of the paper to a level of detail that is necessary to appreciate the results and make sense of them.
   - The full details can be provided either with the code, in appendix, or as supplemental material.

7. **Experiment statistical significance**

   Question: Does the paper report error bars suitably and correctly defined or other appropriate information about the statistical significance of the experiments?

   Answer: [No]

   Justification: In neural combinatorial optimization, we usually adopt the optimality gap and inference time as metrics to measure performance. Both of them are deterministic.

   Guidelines:

   - The answer NA means that the paper does not include experiments.
   - The authors should answer "Yes" if the results are accompanied by error bars, confidence intervals, or statistical significance tests, at least for the experiments that support the main claims of the paper.
   - The factors of variability that the error bars are capturing should be clearly stated (for example, train/test split, initialization, random drawing of some parameter, or overall run with given experimental conditions).

- The method for calculating the error bars should be explained (closed form formula, call to a library function, bootstrap, etc.)
- The assumptions made should be given (e.g., Normally distributed errors).
- It should be clear whether the error bar is the standard deviation or the standard error of the mean.
- It is OK to report 1-sigma error bars, but one should state it. The authors should preferably report a 2-sigma error bar than state that they have a 96% CI, if the hypothesis of Normality of errors is not verified.
- For asymmetric distributions, the authors should be careful not to show in tables or figures symmetric error bars that would yield results that are out of range (e.g. negative error rates).
- If error bars are reported in tables or plots, The authors should explain in the text how they were calculated and reference the corresponding figures or tables in the text.

8. **Experiments compute resources**

   Question: For each experiment, does the paper provide sufficient information on the computer resources (type of compute workers, memory, time of execution) needed to reproduce the experiments?

   Answer: [Yes]

   Justification: We have introduced the hardware used to conduct our experiment in Section. 6. Specifically, we ran our experiments on a single NVIDIA GeForce RTX 3090 GPU with 24GB of memory.

   Guidelines:

   - The answer NA means that the paper does not include experiments.
   - The paper should indicate the type of compute workers CPU or GPU, internal cluster, or cloud provider, including relevant memory and storage.
   - The paper should provide the amount of compute required for each of the individual experimental runs as well as estimate the total compute.
   - The paper should disclose whether the full research project required more compute than the experiments reported in the paper (e.g., preliminary or failed experiments that didn't make it into the paper).

9. **Code of ethics**

   Question: Does the research conducted in the paper conform, in every respect, with the NeurIPS Code of Ethics https://neurips.cc/public/EthicsGuidelines?

   Answer: [Yes]

   Justification: We follow the NeurIPS Code of Ethics in every respect during the research.

   Guidelines:

   - The answer NA means that the authors have not reviewed the NeurIPS Code of Ethics.
   - If the authors answer No, they should explain the special circumstances that require a deviation from the Code of Ethics.
   - The authors should make sure to preserve anonymity (e.g., if there is a special consideration due to laws or regulations in their jurisdiction).

10. **Broader impacts**

    Question: Does the paper discuss both potential positive societal impacts and negative societal impacts of the work performed?

    Answer: [Yes]

    Justification: Yes, we claim the details of societal impacts in the Appendix H. We believe the proposed method has no potential risk of leading to negative impacts that we feel must be highlighted.

    Guidelines:

    - The answer NA means that there is no societal impact of the work performed.

- If the authors answer NA or No, they should explain why their work has no societal impact or why the paper does not address societal impact.
- Examples of negative societal impacts include potential malicious or unintended uses (e.g., disinformation, generating fake profiles, surveillance), fairness considerations (e.g., deployment of technologies that could make decisions that unfairly impact specific groups), privacy considerations, and security considerations.
- The conference expects that many papers will be foundational research and not tied to particular applications, let alone deployments. However, if there is a direct path to any negative applications, the authors should point it out. For example, it is legitimate to point out that an improvement in the quality of generative models could be used to generate deepfakes for disinformation. On the other hand, it is not needed to point out that a generic algorithm for optimizing neural networks could enable people to train models that generate Deepfakes faster.
- The authors should consider possible harms that could arise when the technology is being used as intended and functioning correctly, harms that could arise when the technology is being used as intended but gives incorrect results, and harms following from (intentional or unintentional) misuse of the technology.
- If there are negative societal impacts, the authors could also discuss possible mitigation strategies (e.g., gated release of models, providing defenses in addition to attacks, mechanisms for monitoring misuse, mechanisms to monitor how a system learns from feedback over time, improving the efficiency and accessibility of ML).

11. **Safeguards**

Question: Does the paper describe safeguards that have been put in place for responsible release of data or models that have a high risk for misuse (e.g., pretrained language models, image generators, or scraped datasets)?

Answer: [NA]

Justification: This paper has no such risks.

Guidelines:

- The answer NA means that the paper poses no such risks.
- Released models that have a high risk for misuse or dual-use should be released with necessary safeguards to allow for controlled use of the model, for example by requiring that users adhere to usage guidelines or restrictions to access the model or implementing safety filters.
- Datasets that have been scraped from the Internet could pose safety risks. The authors should describe how they avoided releasing unsafe images.
- We recognize that providing effective safeguards is challenging, and many papers do not require this, but we encourage authors to take this into account and make a best faith effort.

12. **Licenses for existing assets**

Question: Are the creators or original owners of assets (e.g., code, data, models), used in the paper, properly credited and are the license and terms of use explicitly mentioned and properly respected?

Answer: [Yes]

Justification: We cite the creators in the Reference and provide the license of the code in the Appendix. G.

Guidelines:

- The answer NA means that the paper does not use existing assets.
- The authors should cite the original paper that produced the code package or dataset.
- The authors should state which version of the asset is used and, if possible, include a URL.
- The name of the license (e.g., CC-BY 4.0) should be included for each asset.
- For scraped data from a particular source (e.g., website), the copyright and terms of service of that source should be provided.

- If assets are released, the license, copyright information, and terms of use in the package should be provided. For popular datasets, `paperswithcode.com/datasets` has curated licenses for some datasets. Their licensing guide can help determine the license of a dataset.
- For existing datasets that are re-packaged, both the original license and the license of the derived asset (if it has changed) should be provided.
- If this information is not available online, the authors are encouraged to reach out to the asset's creators.

13. **New assets**

Question: Are new assets introduced in the paper well documented and is the documentation provided alongside the assets?

Answer: [NA]

Justification: This paper does not introduce new assets.

Guidelines:

- The answer NA means that the paper does not release new assets.
- Researchers should communicate the details of the dataset/code/model as part of their submissions via structured templates. This includes details about training, license, limitations, etc.
- The paper should discuss whether and how consent was obtained from people whose asset is used.
- At submission time, remember to anonymize your assets (if applicable). You can either create an anonymized URL or include an anonymized zip file.

14. **Crowdsourcing and research with human subjects**

Question: For crowdsourcing experiments and research with human subjects, does the paper include the full text of instructions given to participants and screenshots, if applicable, as well as details about compensation (if any)?

Answer: [NA]

Justification: This paper does not involve crowdsourcing and human subjects.

Guidelines:

- The answer NA means that the paper does not involve crowdsourcing nor research with human subjects.
- Including this information in the supplemental material is fine, but if the main contribution of the paper involves human subjects, then as much detail as possible should be included in the main paper.
- According to the NeurIPS Code of Ethics, workers involved in data collection, curation, or other labor should be paid at least the minimum wage in the country of the data collector.

15. **Institutional review board (IRB) approvals or equivalent for research with human subjects**

Question: Does the paper describe potential risks incurred by study participants, whether such risks were disclosed to the subjects, and whether Institutional Review Board (IRB) approvals (or an equivalent approval/review based on the requirements of your country or institution) were obtained?

Answer: [NA]

Justification: This paper does not involve crowdsourcing and human subjects.

Guidelines:

- The answer NA means that the paper does not involve crowdsourcing nor research with human subjects.
- Depending on the country in which research is conducted, IRB approval (or equivalent) may be required for any human subjects research. If you obtained IRB approval, you should clearly state this in the paper.

- We recognize that the procedures for this may vary significantly between institutions and locations, and we expect authors to adhere to the NeurIPS Code of Ethics and the guidelines for their institution.
- For initial submissions, do not include any information that would break anonymity (if applicable), such as the institution conducting the review.

16. **Declaration of LLM usage**

Question: Does the paper describe the usage of LLMs if it is an important, original, or non-standard component of the core methods in this research? Note that if the LLM is used only for writing, editing, or formatting purposes and does not impact the core methodology, scientific rigorousness, or originality of the research, declaration is not required.

Answer: [Yes]

Justification: We declare our usage of LLM in Section. 5, which involved in designing projection strategies.

Guidelines:

- The answer NA means that the core method development in this research does not involve LLMs as any important, original, or non-standard components.
- Please refer to our LLM policy (`https://neurips.cc/Conferences/2025/LLM`) for what should or should not be described.

A   Related work

A.1   Review for Non-Constructive Method

Despite direct learning to construct a VRP solution, other methods work closely with search and improvement methods [63–65]. Early studies [66] utilize a graph convolutional network to generate heatmaps indicating the probability of edges belonging to optimal solutions for TSP instances. Subsequently, an approximate solution can be obtained via beam search [66], Monte Carlo tree search [19], dynamic programming [67], and guided local search [68]. While initially developed for small-scale problems, recent studies extend heatmap-based methods to larger TSP instances [19, 69]. However, the adaptability of these methods can be limited by their reliance on carefully tuned search strategies. Furthermore, the heatmap representation primarily focuses on edge probabilities, which may restrict applicability to problems with complex constraints.

Another research direction involves learning-augmented algorithms, where neural networks enhance traditional heuristic solvers. This includes accelerating solvers by learning operation selection [63, 70, 71], guided improvement [72–74], and problem decomposition [45, 75]. Many improvement-based methods propose to iteratively refine feasible solutions [76, 77, 70]. Nonetheless, these methods typically depend on well-designed heuristic operators or advanced solvers [78, 57] for solving different problems.

A.2   Review for LLM-AHD Method

Recent advancements demonstrate the significant potential of Large Language Models (LLMs) in automating the design of high-performing heuristics for complex computational problems. This methodology typically involves maintaining a population of elite heuristic functions, which are evaluated and ranked based on their fitness on a designated dataset. The LLM is then iteratively prompted with high-performing functions from this population to generate potentially superior heuristic candidates. EoH [52] and Funsearch [79] pioneer the application of LLM to design a population-based evolutionary computation procedure. Building on this, ReEvo [80] incorporates a reflection mechanism to augment the LLM's reasoning capabilities during heuristic generation. Addressing the challenge of premature convergence, HSEvo [81] introduces diversity metrics and a harmony search algorithm to enhance population diversity without degrading solution quality. In a different approach, MCTS-AHD [53] conceptualizes the task as a search problem, modeling the heuristic design process as a Monte Carlo tree search to systematically explore the solution space.

B   Detailed Methodology

In TSP instances, the input distribution can be interpreted as the coordinate distribution, and transforming the coordinate to a uniform distribution can be seen as normalization. To ease the understanding, we replace the projection with normalization when prompting the LLM. While the input of CVRP instances has extra demand and capacity, changing these features can easily lead to unfeasible solutions. Consequently, we limit the modification to input within custom node coordinates, and the projection can be similarly interpreted as normalization.

B.1   Prompts of TTPL

Our LLM-driven prompt framework for projection evolution consists of four core strategies (E1, E2, M1, M2) [52], each structured around three components: **task description**, **strategy-specific instructions**, **parent projection**, and **template program**. In the following, we detail their design principles:

- **E1 (Exploratory Generation):** This prompt instructs an LLM to generate entirely new projection strategies by contrasting two existing approaches, explicitly avoiding structural similarities. It emphasizes divergence, requiring the LLM to innovate beyond the provided examples.

Prompt for E1

I need help designing an innovative coordinate normalization strategy function implemented in PyTorch to normalize a set of nodes' coordinates, aiming to maximize the final negative gap. The input is a tensor with shape (batch, num_nodes, 2) and the 'all_coors' must be a tensor with the same shape as 'coor1'.

I have 2 existing algorithms with their codes as follows:
No. 1 algorithm and the corresponding code are:
{projection description}
{Code}
No. 2 algorithm and the corresponding code are:
{projection description}
{Code}

Please help me create a new algorithm that has a completely different form from the given ones.
1. First, describe your new algorithm and main steps in one sentence. The description must be within boxed {}.
2. Next, implement the following Python function:
{Template Projection}

- **E2 (Backbone-Driven Innovation):** Focused on identifying common design principles across parent strategies, this prompt guides an LLM to extract shared computational patterns (e.g., scaling mechanisms, coordinate transformations) and generate variants that preserve these core ideas while introducing novel components.

Prompt for E2

I need help designing an innovative coordinate normalization strategy function implemented in PyTorch to normalize a set of nodes' coordinates, aiming to maximize the final negative gap. The input is a tensor with shape (batch, num_nodes, 2) and the 'all_coors' must be a tensor with the same shape as 'coor1'.

I have 2 existing algorithms with their codes as follows:
No. 1 algorithm and the corresponding code are:
{Projection description}
{Code}
No. 2 algorithm and the corresponding code are:
{Projection description}
{Code}

Please help me create a new algorithm that has a completely different form from the given ones, but can be motivated by them.
1. Firstly, identify the common backbone idea in the provided algorithms.
2. Secondly, based on the backbone idea, describe your new algorithm in one sentence. The description must be within boxed {}.
3. Thirdly, implement the following Python function:
{Template Projection}

- **M1 (Structural Mutation):** Targets architectural modifications by presenting a single parent strategy and prompting an LLM to redesign its core operations (e.g., changing anchor point for reference).

23

- **M2 (Parametric Optimization):** Specializes in parameter tuning for critical projection variables (e.g., scaling factors, shift coefficients), directing an LLM to systematically adjust numerical settings.

The prompt engineering for normalization evolution adopts a standardized template structure across strategies. The template code for TSP and CVRP builds on the INViT framework [15].

Template Program for TSP

```python
def normalize(coor1: torch.Tensor) -> torch.Tensor:
    """
    Args:
        coor1: coordinates of nodes, shape: (batch, 1+k+1, 2)

    Return:
        all_coors: a tensor containing normalized coordinates, same shape as
    coor1

    Note:
        first_node: coor1[:,[0],:], left_node: coor1[:,1:-1,:], last_node:
    [:,[-1],:]
        left_node is the topk close to the last_node
    """
    batch_size = coor1.shape[0]
    all_coors = coor1
    graph = all_coors[:, 1:, :]
    min_values = torch.reshape(torch.min(graph, 1).values, (batch_size, 1, 2)
    )
    all_coors = all_coors - min_values  # translate
    ratio_x = torch.reshape(
        torch.max(graph[:, :, 0], 1).values - torch.min(graph[:, :, 0], 1).
    values,
        (-1, 1),
    )
    ratio_y = torch.reshape(
        torch.max(graph[:, :, 1], 1).values - torch.min(graph[:, :, 1], 1).
    values,
        (-1, 1),
    )
    ratio = torch.max(torch.cat((ratio_x, ratio_y), 1), 1).values
    ratio[ratio == 0] = 1
    all_coors = all_coors / (torch.reshape(ratio, (batch_size, 1, 1)))
    all_coors[ratio == 0, :, :] = (
        all_coors[ratio == 0, :, :] + min_values[ratio == 0, :, :]
    )
    all_coors = torch.clip(all_coors, 0, 1)
    return all_coors
```

Task Description for CVRP

I need to develop a coordinate normalization method for CVRP sequences that preserves critical geometric relationships between nodes while enabling effective neural network processing. The function should take depot/vehicle coordinates (coor1), customer node (coor2), and final stop coordinates (coor3) as PyTorch tensors, maintaining their original shapes. Key objectives are: 1) Establish spatial consistency across batches without distorting relative positions, 2) Use the initial node as an anchor point for stable reference, 3) Prevent information loss from hard clipping while controlling magnitude variance, and 4) Ensure scale-invariant features that help the downstream model generalize across problem sizes. The solution should particularly focus on maintaining directional relationships and proportional distances rather than absolute positional constraints.

Template Program for CVRP

```python
def normalize(
    coor1: torch.Tensor, coor2: torch.Tensor, coor3: torch.Tensor
) -> torch.Tensor:
    """
    Args:
        coor1: indicate the first node, shape: (batch, 1, 2)
        coor2: coordinates of the rest of nodes, shape: (batch, 100, 2)
        coor3: coordinate of the last node, shape: (batch, 1, 2)

    Return:
        coor1: normalized coordinate of the first node, shape: (batch, 1, 2)
        coor2: normalized coordinates of the rest of nodes, shape: (batch,
    left_num, 2)
        coor3: normalized coordinate of the last node, shape: (batch, 1, 2)
    """
    lengths = [coor1.shape[1], coor2.shape[1], coor3.shape[1]]
    all_coors = torch.cat((coor1, coor2, coor3), dim=1)
    last_neighbors_xy = all_coors[:, 1:, :]
    # shape: (batch, 1+neighbor_k, 2)
    xy_max = torch.max(last_neighbors_xy, dim=1, keepdim=True).values
    xy_min = torch.min(last_neighbors_xy, dim=1, keepdim=True).values
    # shape: (batch, 1, 2)
    ratio = torch.max((xy_max - xy_min), dim=-1, keepdim=True).values
    ratio[ratio == 0] = 1
    # shape: (batch, 1, 1)
    all_coors = torch.clip((all_coors - xy_min) / ratio.expand(-1, 1, 2), 0,
    1)
    coor1, coor2, coor3 = torch.split(all_coors, lengths, dim=1)
    return coor1, coor2, coor3
```

B.2 EoH Algorithm

The EoH is a population-based framework for LLM-based AHD [52]. The algorithm optimizes heuristics by iteratively applying LLM-guided mutation, crossover, and selection operations, enabling the exploration of diverse heuristic designs.

EoH begins by initializing a population of N heuristics using LLM, where each heuristic is evaluated on dataset D to compute its fitness value f. In each generation, five evolution strategies (E1, E2, M1, M2, M3) are used to generate new heuristics. For each strategy, N parent heuristics are sampled from the current population using rank-based probabilities. LLMs then generate new heuristics by mutating or combining features from the parents, guided by the evolution strategy. New candidates are evaluated in D, and feasible ones are added to a candidate pool after removing duplicates. Finally, the top N heuristics of the expanded pool are selected to form the next generation. This process repeats for N_g generations, eventually returning the heuristic with the highest fitness. The pseudo-code for the EoH is provided in the Algorithm 2.

Algorithm 2 Evolution of heuristics for automatic heuristic design

1: **Input:**
2:    Population size N, Max generations N_g, Evaluation dataset D, Evaluation function f.
3: **Output:**
4:    The best found heuristic h^*.
5: **Step 0: Initialization**
6: **for** $j = 1 : N$ **do**
7:    Generate heuristic h_j using initialization prompt.
8:    Evaluate h_j on D to obtain fitness $f(D, h_j)$.
9: **end for**
10: Build initial population $P_0 \leftarrow \{h_1, ..., h_N\}$.
11: Set $O \leftarrow P_0$.
12: **Step 1: Generation of Heuristics**
13: **for** $i = 1 : N_g$ **do**
14:    Rank P_{i-1} by fitness $\rightarrow \{r_1, ..., r_N\}$.
15:    **for** $S \in \{E1, E2, M1, M2, M3\}$ **do**
16:       **for** $j = 1 : N$ **do**
17:          Sample parents from P_{i-1} via rank-based sampling.
18:          Generate new heuristic h_j based parents using evolution strategies S.
19:          Evaluate h_j on the evaluation dataset D and obtain the fitness value $f_\theta(D, h_j)$.
20:          **if** h_j is feasible **then**
21:             Add h_j to candidate pool O
22:          **end if**
23:       **end for**
24:    **end for**
25:    Remove duplicates in O.
26:    **Step 2: Population Management**
27:    Sort O in descending order based on their fitness value.
28:    Update P_i with the first N heuristics in O.
29: **end for**
30: **return** Heuristic h^* with the highest fitness in the final population.

C TTPL Designed Strategies

C.1 TSP Instances

In this section, we present representative projection strategies optimized by TTPL for TSP and CVRP instances. For TSP, the input is the coordinates of the nodes in the KNN subgraph, and the output is the corresponding transformed coordinates. For CVRP, the inputs consist of the coordinates of the depot, the current node, and the coordinates of the nodes in the KNN subgraph, and the output is the transformed coordinates of these nodes.

For TSP1K instances, TTPL evolves the following projection:

Code 1: Projection designed by TTPL on TSP1K

```python
def normalize(coor1: torch.tensor) -> torch.tensor:

    batch_size = coor1.shape[0]
    all_coors = coor1
    graph = all_coors[:, 1:, :]

    # Translate to the maximum values
    max_values = torch.reshape(torch.max(graph, dim=1).values, (batch_size, 1, 2))
    all_coors = max_values - all_coors  # translate

    # Calculate ranges for normalization
    ratio_x = torch.reshape(torch.max(graph[:, :, 0], dim=1).values - torch.min(
    graph[:, :, 0], dim=1).values, (-1, 1))
    ratio_y = torch.reshape(torch.max(graph[:, :, 1], dim=1).values - torch.min(
    graph[:, :, 1], dim=1).values, (-1, 1))

    # Find the maximum scale factor
    ratio = torch.max(torch.cat((ratio_x, ratio_y), dim=1), dim=1).values
    ratio[ratio == 0] = 1  # Avoid division by zero

    # Normalize the coordinates
    all_coors = all_coors / (torch.reshape(ratio, (batch_size, 1, 1)))
    all_coors[ratio == 0, :, :] = all_coors[ratio == 0, :, :] + max_values[ratio ==
    0, :, :]

    # Clip to ensure values are within [0, 1]
    all_coors = torch.clip(all_coors, 0, 1)

    return all_coors
```

The corresponding mathematical formulation proceeds as follows. Given input coordinates $S = \{s_0, s_1, \ldots, s_N\}$ where $s_i \in \mathbb{R}^2$, with s_i^x and s_i^y denoting the component of s_i, the projection process proceeds as follows:

$$M = \left(\max_{1 \leq j \leq N} s_j^x, \ \max_{1 \leq j \leq N} s_j^y \right).$$

The next step is to establish the maximum coordinate values $M = (M_x, M_y)$ as the reference point for transformations, which can be formulated as:

$$\widetilde{S} = \{\widetilde{s}_i \mid \widetilde{s}_i = M - s_i, \ \forall i \in \{0, \ldots, N\}\}.$$

Then, mirrored coordinates are created by reflecting points about the reference point M, ensuring all coordinates lie in the positive quadrant

$$r_x = \max_{1 \leq j \leq N} s_j^x - \min_{1 \leq j \leq N} s_j^x,$$
$$r_y = \max_{1 \leq j \leq N} s_j^y - \min_{1 \leq j \leq N} s_j^y.$$

Moreover, the coordinate ranges are calculated along both axes to determine the scaling factor

$$r = \begin{cases} \max(r_x, r_y) & \text{if } \max(r_x, r_y) > 0, \\ 1 & \text{otherwise.} \end{cases}$$

Such that, the maximum range is selected as the normalization factor, with special handling for zero-range edge cases

$$\widehat{S} = \left\{ \widehat{s}_i \,\middle|\, \widehat{s}_i = \frac{\widetilde{s}_i}{r} + M, \; \forall i \in \{0, \dots, N\} \right\}.$$

Finally, coordinates are normalized to [0,1] relative to the reference point while preserving spatial relationships, and final coordinates are ensured to reside within the unit square through clipping operations, completing the projection

$$\widehat{S}_{clipped} = \left\{ (\min(\max(\widehat{s}_i^x, 0), 1), \min(\max(\widehat{s}_i^y, 0), 1)), \; \forall i \in \{0, \dots, N\} \right\}.$$

For TSP5K instances, the evolved projection strategy is implemented as:

Code 2: Projection designed by TTPL on TSP5K

```python
def normalize(coor1: torch.tensor) -> torch.tensor:

    batch_size = coor1.shape[0]
    all_coors = coor1
    graph = all_coors[:, 1:, :]

    # Translate by the minimum values in the graph
    min_values = torch.reshape(torch.min(graph, 1).values, (batch_size, 1, 2))
    all_coors = all_coors - min_values  # translate

    # Apply a non-linear transformation
    all_coors = torch.tanh(all_coors)

    # Calculate scaling ratios with a slight modification
    ratio_x = torch.reshape(torch.max(graph[:, :, 0], 1).values - torch.min(graph[:,
     :, 0], 1).values, (-1, 1))
    ratio_y = torch.reshape(torch.max(graph[:, :, 1], 1).values - torch.min(graph[:,
     :, 1], 1).values, (-1, 1))
    ratio = torch.max(torch.cat((ratio_x, ratio_y), 1), 1).values

    # Avoid division by zero
    ratio[ratio == 0] = 1
    all_coors = all_coors / (torch.reshape(ratio, (batch_size, 1, 1)))

    # Post-process coordinates to ensure they are clipped within [0, 1]
    all_coors = torch.clip(all_coors, 0, 1)

    return all_coors
```

The projection process follows these operations:

$$M = \left(\min_{1 \le j \le N} s_j^x, \; \min_{1 \le j \le N} s_j^y \right)$$

$$\widetilde{S} = \{ \widetilde{s}_i \mid \widetilde{s}_i = s_i - M, \; \forall i \in \{0, \dots, N\} \}$$

$$\widetilde{S} = \{ (\tanh(\widetilde{s}_i^x), \tanh(\widetilde{s}_i^y)), \; \forall i \in \{0, \dots, N\} \}$$

The hyperbolic tangent function is employed to compress coordinates into (-1,1) while preserving spatial relationships. The detailed operations are listed as follows:

$$r_x = \max_{1 \le j \le N} s_j^x - \min_{1 \le j \le N} s_j^x,$$

$$r_y = \max_{1 \le j \le N} s_j^y - \min_{1 \le j \le N} s_j^y,$$

$$r = \begin{cases} \max(r_x, r_y) & \text{if } \max(r_x, r_y) > 0, \\ 1 & \text{otherwise,} \end{cases}$$

$$\widehat{S} = \left\{ \widehat{s}_i \mid \widehat{s}_i = \frac{\widetilde{s}_i}{r}, \ \forall i \in \{0, \ldots, N\} \right\},$$

$$\widehat{S} = \left\{ (\min(\max(\widehat{s}_i^x, 0), 1), \min(\max(\widehat{s}_i^y, 0), 1)), \ \forall i \in \{0, \ldots, N\} \right\}.$$

For TSP10K instances, TTPL generates this projection:

Code 3: Projection designed by TTPL on TSP10K

```python
def normalize(coor1):

    batch_size = coor1.shape[0]
    all_coors = coor1.clone()
    graph = all_coors[:, 1:, :]

    # Step 1: Calculate midpoints for translation
    midpoints = (torch.max(graph, 1).values + torch.min(graph, 1).values) / 2
    midpoints = torch.reshape(midpoints, (batch_size, 1, 2))
    all_coors = all_coors - midpoints  # translate

    # Step 2: Calculate the new range after translation
    range_x = torch.reshape(torch.max(graph[:, :, 0], 1).values - torch.min(graph[:,
     :, 0], 1).values, (-1, 1))
    range_y = torch.reshape(torch.max(graph[:, :, 1], 1).values - torch.min(graph[:,
     :, 1], 1).values, (-1, 1))
    range_val = torch.max(torch.cat((range_x, range_y), 1), 1).values
    range_val[range_val == 0] = 1  # Prevent division by zero

    # Step 3: Scale coordinates
    all_coors = all_coors / (torch.reshape(range_val, (batch_size, 1, 1 )))

    # Step 4: Shift values to center in [0, 1]
    all_coors = (all_coors + 0.5)

    # Step 5: Clip the values to [0, 1]
    all_coors = torch.clamp(all_coors, 0, 1)

    return all_coors
```

It first calculates the centroid of the input coordinates using the average of extreme values:

$$M = \left(\frac{\max\limits_{1 \le j \le N} s_j^x + \min\limits_{1 \le j \le N} s_j^x}{2}, \frac{\max\limits_{1 \le j \le N} s_j^y + \min\limits_{1 \le j \le N} s_j^y}{2} \right).$$

Then, the projection is mathematically written below:

$$\widetilde{S} = \{\widetilde{s}_i \mid \widetilde{s}_i = s_i - M, \ \forall i \in \{0, \ldots, N\}\},$$

$$r_x = \max_{1 \leq j \leq N} s_j^x - \min_{1 \leq j \leq N} s_j^x,$$

$$r_y = \max_{1 \leq j \leq N} s_j^y - \min_{1 \leq j \leq N} s_j^y,$$

$$r = \begin{cases} \max(r_x, r_y) & \text{if } \max(r_x, r_y) > 0, \\ 1 & \text{otherwise,} \end{cases}$$

$$\widehat{S} = \left\{ \widehat{s}_i \ \middle| \ \widehat{s}_i = \frac{\widetilde{s}_i}{r}, \ \forall i \in \{0, \ldots, N\} \right\},$$

$$\widehat{S} = \widehat{S} + (0.5, 0.5),$$

$$\widehat{S}_{clipped} = \left\{ (\min(\max(\widehat{s}_i^x, 0), 1), \min(\max(\widehat{s}_i^y, 0), 1)), \ \forall i \in \{0, \ldots, N\} \right\}.$$

C.2 CVRP Instances

For CVRP instances, TTPL develops specialized strategies to handle depot-customer relationships. The CVRP1K projection strategy is implemented via:

Code 4: Projection designed by TTPL on CVRP1K

```python
def normalize(coor1: torch.Tensor, coor2: torch.Tensor, coor3: torch.Tensor) ->
    torch.Tensor:

    lengths = [coor1.shape[1], coor2.shape[1], coor3.shape[1]]
    all_coors = torch.cat((coor1, coor2, coor3), dim=1)

    # Calculate the relative vectors
    relative_vectors = all_coors - coor1

    # Compute the magnitudes of the vectors
    magnitudes = torch.norm(relative_vectors, dim=-1, keepdim=True)

    # Avoid division by zero
    magnitudes[magnitudes == 0] = 1

    # Normalize the vectors to unit vectors
    unit_vectors = relative_vectors / magnitudes

    # Scale unit vectors by the normalized magnitudes
    normalized_vectors = unit_vectors * (magnitudes / magnitudes.max(dim=1, keepdim=
    True).values)

    # Combine normalized vectors with the anchor point
    normalized_coors = coor1 + normalized_vectors

    coor1, coor2, coor3 = torch.split(normalized_coors, lengths, dim=1)

    return coor1, coor2, coor3
```

The projection first integrates all coordinates into a unified set with depot s_0 as the reference origin

$$v_i = s_i - s_0, \quad \forall i \in \{0, \ldots, N\}.$$

Secondly, position vectors are computed relative to the depot, establishing translation-invariant representations

$$\|v_i\| = \begin{cases} \sqrt{v_i^{x2} + v_i^{y2}} & \text{if } \sqrt{v_i^{x2} + v_i^{y2}} > 0, \\ 1 & \text{otherwise.} \end{cases}$$

Thirdly, vector magnitudes are computed with zero-division protection to ensure numerical stability

$$\widehat{v}_i = \frac{v_i}{\|v_i\|} \odot \frac{\|v_i\|}{\max\limits_{0 \le j \le N} \|v_j\|}.$$

Furthermore, magnitude scaling is performed relative to the maximum vector length

$$\widehat{s}_i = s_0 + \widehat{v}_i.$$

Then, absolute coordinates are reconstructed while maintaining spatial relationships

$$\widehat{S}_f = \{\widehat{s}_0\}, \quad \widehat{S}_k = \{\widehat{s}_1, \ldots, \widehat{s}_{N-1}\}, \quad \widehat{S}_l = \{\widehat{s}_N\}.$$

Finally, given coordinate sets $S_f = \{s_0\}$ (depot), $S_k = \{s_1, \ldots, s_{N-1}\}$, and $S_l = \{s_N\}$ where $s_i \in \mathbb{R}^2$, the normalized coordinates $\widehat{S}_f, \widehat{S}_k, \widehat{S}_l$ are computed through:

$$S = S_f \cup S_k \cup S_l = \{s_0, s_1, \ldots, s_N\}$$

For CVRP5K instances, the evolved projection strategy is implemented as:

Code 5: Projection designed by TTPL on CVRP5K

```python
def normalize(coor1: torch.Tensor, coor2: torch.Tensor, coor3: torch.Tensor) ->
    torch.Tensor:

    lengths = [coor1.shape[1], coor2.shape[1], coor3.shape[1]]
    all_coors = torch.cat((coor1, coor2, coor3), dim=1)

    # Get anchor point (coor1)
    anchor = coor1

    # Translate coordinates based on the anchor
    translated_coors = all_coors - anchor

    # Calculate distances to the anchor point
    distances = torch.norm(translated_coors, p=2, dim=-1, keepdim=True)

    # Find the furthest distance for scaling
    farthest_distance, _ = distances.max(dim=1, keepdim=True)
    scaling_factor = torch.sqrt(farthest_distance)

    scaling_factor[scaling_factor == 0] = 1  # Prevent division by zero

    # Normalize the coordinates using the scaling factor
    normalized_coors = translated_coors / scaling_factor.expand_as(translated_coors)

    # Combine back with the anchor
    normalized_coors += anchor

    # Split back to original coordinates
    coor1, coor2, coor3 = torch.split(normalized_coors, lengths, dim=1)

    return coor1, coor2, coor3
```

The projection steps are formalized by:

$$v_i = s_i - s_0, \quad \forall i \in \{0, \ldots, N\},$$

$$\|v_i\| = \sqrt{v_i^{x2} + v_i^{y2}},$$

$$v_{\max} = \begin{cases} \sqrt{\max\limits_{0 \leq j \leq N} \|v_j\|} & \text{if } \sqrt{\max\limits_{0 \leq j \leq N} \|v_j\|} > 0, \\ 1 & \text{otherwise,} \end{cases}$$

$$\widehat{v}_i = \frac{v_i}{v_{\max}},$$

$$\widehat{s}_i = s_0 + \widehat{v}_i,$$

$$\widehat{S}_f = \{\widehat{s}_0\}, \quad \widehat{S}_k = \{\widehat{s}_1, \ldots, \widehat{s}_{N-1}\}, \quad \widehat{S}_l = \{\widehat{s}_N\},$$

$$S = S_f \cup S_k \cup S_l = \{s_0, s_1, \ldots, s_N\}.$$

For CVRP10K instances, TTPL generates this projection:

Code 6: Projection designed by TTPL on CVRP10K

```python
def normalize(coor1: torch.Tensor, coor2: torch.Tensor, coor3: torch.Tensor) ->
    torch.Tensor:

    lengths = [coor1.shape[1], coor2.shape[1], coor3.shape[1]]
    all_coors = torch.cat((coor1, coor2, coor3), dim=1)

    # Centering the coordinates around the first node
    center = coor1.squeeze(1)  # shape: (batch, 2)
    relative_coors = all_coors - center.unsqueeze(1)  # shape: (batch, 1 + k, 2)

    # Calculate distances from the first node
    distances = torch.norm(relative_coors, dim=-1, keepdim=True)  # shape: (batch, 1
     + k, 1)

    # Apply a non-linear transformation to the distances (e.g., exponential scaling)
    transformed_distances = torch.exp(distances) - 1  # shape: (batch, 1 + k, 1)

    # Scale transformed distances to [0, 1]
    max_distance = torch.max(transformed_distances, dim=1, keepdim=True).values
    max_distance[max_distance == 0] = 1  # Prevent division by zero
    normalized_distances = transformed_distances / max_distance  # shape: (batch, 1
    + k, 1)

    # Maintain direction by re-constructing relative coordinates
    direction = relative_coors / (distances + 1e-6)  # shape: (batch, 1 + k, 2)
    normalized_coors = normalized_distances * direction  # shape: (batch, 1 + k, 2)

    all_coors = normalized_coors + center.unsqueeze(1)  # Translate back to original
     position

    coor1, coor2, coor3 = torch.split(all_coors, lengths, dim=1)

    return coor1, coor2, coor3
```

The projection process follows these operations:

$$v_i = s_i - s_0, \quad \forall i \in \{0, \ldots, N\},$$

$$\|v_i\| = \sqrt{v_i^{x2} + v_i^{y2}},$$

$$\widetilde{v}_i = e^{\|v_i\|} - 1,$$

$$v_{\max} = \begin{cases} \max_{0 \le j \le N} \widetilde{v}_j & \text{if } \max_{0 \le j \le N} \widetilde{v}_j > 0, \\ 1 & \text{otherwise}, \end{cases}$$

$$v_i = \frac{\widetilde{v}_i}{v_{\max}},$$

$$\widehat{v}_i = \frac{\widetilde{v}_i}{v_{\max}} \odot \frac{v_i}{\|v_i\| + 1e6},$$

$$\widehat{s}_i = s_0 + \widehat{v}_i,$$

$$\widehat{S}_f = \{\widehat{s}_0\}, \quad \widehat{S}_k = \{\widehat{s}_1, \ldots, \widehat{s}_{N-1}\}, \quad \widehat{S}_l = \{\widehat{s}_N\},$$

$$S = S_f \cup S_k \cup S_l = \{s_0, s_1, \ldots, s_N\}.$$

D Experiment Details

D.1 TSPLIB and CVRPLIB Results

We evaluate the proposed method in four benchmark scenarios: TSPLIB [59] and CVRPLib [60] instances with comparisons in both greedy and post-search frameworks. We compare our method against five baselines: INViT [15], SIGD [62], BQ [42], LEHD [18] and GLOP [13]. For TSPLIB, all experiments are conducted on large-scale instances ranging from 1,000 to 85,900 nodes to assess scalability and generalization.

As shown in the Table. 7, our method achieves a 3.88% average optimality gap across all 33 instances, significantly reducing the optimality gap by 64.86%, 92.02%, 94.00%, and 78.10% compared with INViT, SIGD greedy, BQ greedy, and LEHD greedy.

Table 7: Optimality gaps of greedy-based NCO methods on TSPLib instances. "OOM" signifies out-of-memory failures. Solved# and average gaps are summarized at the bottom.

Instance	Scale	INViT	SIGD greedy	BQ greedy	LEHD greedy	Ours
dsj1000	1,000	9.20%	7.82%	6.96%	8.31%	**2.40%**
pr1002	1,002	16.43%	2.95%	3.35%	4.44%	**0.90%**
u1060	1,060	12.29%	7.60%	10.72%	10.00%	**1.22%**
vm1084	1,084	10.91%	**3.38%**	4.41%	5.42%	4.32%
pcb1173	1,173	8.67%	4.32%	5.61%	8.01%	**2.25%**
d1291	1,291	22.37%	4.50%	10.93%	14.13%	**3.59%**
rl1304	1,304	8.90%	**3.18%**	8.48%	8.14%	3.76%
rl1323	1,323	17.02%	**3.64%**	5.44%	9.26%	5.56%
nrw1379	1,379	5.25%	27.91%	18.96%	15.49%	**1.00%**
fl1400	1,400	18.30%	24.87%	16.73%	18.80%	**7.91%**
u1432	1,432	6.16%	**2.79%**	4.65%	7.96%	2.81%
fl1577	1,577	12.63%	22.37%	19.95%	14.68%	**4.97%**
d1655	1,655	12.81%	14.55%	12.53%	13.89%	**5.57%**
vm1748	1,748	16.27%	9.95%	7.71%	10.10%	**2.37%**
u1817	1,817	7.31%	7.29%	8.40%	10.32%	**4.72%**
rl1889	1,889	10.44%	7.30%	7.93%	7.49%	**5.70%**
d2103	2,103	16.79%	10.46%	16.48%	14.57%	**5.78%**
u2152	2,152	10.38%	10.22%	11.56%	12.65%	**4.01%**
u2319	2,319	0.98%	3.73%	4.33%	4.18%	**0.31%**
pr2392	2,392	8.29%	8.88%	13.96%	12.33%	**3.53%**
pcb3038	3,038	6.85%	11.01%	17.33%	13.44%	**3.55%**
fl3795	3,795	18.75%	57.46%	30.97%	13.55%	**9.29%**
fnl4461	4,461	7.32%	28.33%	20.35%	19.05%	**2.16%**
rl5915	5,915	14.02%	44.31%	26.77%	24.17%	**4.48%**
rl5934	5,934	12.91%	53.73%	33.19%	24.11%	**4.26%**
pla7397	7,397	9.45%	90.16%	69.34%	40.94%	**5.42%**
rl11849	11,849	12.71%	105.26%	46.65%	38.04%	**4.86%**
usa13509	13,509	13.44%	525.78%	676.67%	71.10%	**4.55%**
brd14051	14,051	9.31%	138.65%	145.41%	41.22%	**3.98%**
d15112	15,112	7.24%	145.56%	172.38%	35.82%	**2.09%**
d18512	18,512	6.62%	119.58%	126.51%	OOM	**1.97%**
pla33810	33,810	7.04%	OOM	504.13%	OOM	**5.34%**
pla85900	85,900	7.21%	OOM	OOM	OOM	**3.54%**
Sloved#		33/33	31/33	32/33	30/33	33/33
Avg.gap		11.04%	48.63%	64.65%	17.72%	**3.88%**

As shown in the Table 8, our method achieves a 1.37% average optimality gap across all 33 TSPLIB instances under the post-search framework, reducing the gap by 88.03%, 89.43%, 81.41%, and 75.09% compared to SIGD bs16, BQ bs16, LEHD RRC1000, and GLOP, respectively.

Table 8: Optimality gaps of post-search-based NCO methods on TSPLIB instances.

Instance	Scale	SIGD bs16	BQ bs16	LEHD RRC1000	GLOP	Ours RRC1000
dsj1000	1,000	9.27%	4.35%	2.45%	2.45%	**0.63%**
pr1002	1,002	2.25%	2.04%	1.08%	3.02%	**0.14%**
u1060	1,060	5.45%	5.82%	2.79%	2.40%	**0.27%**
vm1084	1,084	6.68%	5.48%	1.47%	3.83%	**0.24%**
pcb1173	1,173	2.61%	4.45%	2.99%	5.92%	**0.63%**
d1291	1,291	6.85%	7.38%	2.88%	5.78%	**1.16%**
rl1304	1,304	3.64%	6.30%	3.14%	8.02%	**0.12%**
rl1323	1,323	2.24%	4.51%	1.16%	6.27%	**0.51%**
nrw1379	1,379	17.82%	13.23%	8.34%	3.34%	**0.39%**
fl1400	1,400	33.75%	37.48%	2.96%	2.15%	**1.14%**
u1432	1,432	2.10%	4.25%	2.24%	3.40%	**0.67%**
fl1577	1,577	33.27%	18.32%	3.81%	5.85%	**1.19%**
d1655	1,655	12.98%	10.20%	5.09%	5.33%	**2.36%**
vm1748	1,748	4.59%	6.42%	3.36%	3.75%	**0.39%**
u1817	1,817	5.91%	6.07%	4.83%	6.26%	**2.61%**
rl1889	1,889	7.39%	7.24%	3.17%	7.06%	**1.25%**
d2103	2,103	12.66%	15.46%	2.14%	9.58%	**0.13%**
u2152	2,152	7.11%	7.69%	6.22%	7.32%	**1.77%**
u2319	2,319	1.42%	3.17%	1.47%	1.29%	**0.19%**
pr2392	2,392	5.68%	10.53%	5.63%	5.20%	**0.76%**
pcb3038	3,038	6.56%	11.51%	7.49%	5.28%	**1.32%**
fl3795	3,795	53.43%	38.33%	6.85%	7.45%	**5.05%**
fnl4461	4,461	19.22%	14.68%	10.37%	4.47%	**1.10%**
rl5915	5,915	OOM	19.58%	12.38%	10.35%	**1.76%**
rl5934	5,934	OOM	24.53%	11.94%	10.28%	**1.99%**
pla7397	7,397	OOM	47.63%	15.31%	5.94%	**2.68%**
rl11849	11,849	OOM	OOM	18.19%	8.69%	**2.48%**
usa13509	13,509	OOM	OOM	31.37%	5.32%	**1.85%**
brd14051	14,051	OOM	OOM	21.19%	4.73%	**2.47%**
d15112	15,112	OOM	OOM	18.83%	4.67%	**1.06%**
d18512	18,512	OOM	OOM	OOM	4.98%	**1.15%**
pla33810	33,810	OOM	OOM	OOM	OOM	**3.37%**
pla85900	85,900	OOM	OOM	OOM	OOM	**2.43%**
Sloved#		23/33	26/33	30/33	31/33	33/33
Avg.gap		11.43%	12.95%	7.37%	5.50%	**1.37%**

For CVRPLIB, we evaluate both greedy and post-search frameworks on large-scale instances ranging from 1,000 to 30,000 nodes. As shown in the Table. 9 and Table. 10, our method achieves 10.97% and 7.34% average optimality gaps in the greedy and post-search frameworks, respectively, outperforming all baselines in both settings.

Table 9: Optimality gaps of greedy-based NCO methods on CVRPLIB instances.

Instance	Scale	INViT	SIGD greedy	BQ greedy	LEHD greedy	Ours
X-n1001-k43	1,000	12.60%	8.02%	4.99%	7.57%	**4.95%**
Li_30	1,040	**9.12%**	9.81%	10.62%	12.54%	12.84%
Li_31	1,120	12.42%	12.88%	12.93%	**4.95%**	16.12%
Li_32	1,200	9.90%	13.61%	13.48%	**7.68%**	11.30%
Leuven1	3,000	13.71%	16.19%	18.53%	16.60%	**5.69%**
Leuven2	4,000	26.08%	25.64%	30.70%	34.85%	**14.99%**
Antwerp1	6,000	15.40%	13.98%	16.48%	14.66%	**5.76%**
Antwerp2	7,000	27.75%	17.72%	27.67%	22.77%	**11.66%**
Ghent1	10,000	15.87%	24.22%	25.36%	27.23%	**5.73%**
Ghent2	11,000	30.78%	28.09%	54.04%	38.36%	**15.56%**
Brussels1	15,000	18.09%	25.48%	35.70%	OOM	**6.80%**
Brussels2	16,000	32.08%	38.32%	50.90%	OOM	**15.38%**
Flanders1	20,000	23.41%	43.95%	37.51%	OOM	**7.35%**
Flanders2	30,000	39.60%	136.89%	110.09%	OOM	**19.43%**
Sloved#		14/14	14/14	14/14	10/14	14/14
Avg.gap		20.49%	29.63%	32.07%	18.72%	**10.97%**

Table 10: Optimality gaps of post-search-based NCO methods on CVRPLIB instances.

Instance	Scale	SIGD bs16	BQ bs16	LEHD RRC1000	GLOP	Ours RRC1000
X-n1001-k43	1,000	5.68%	3.07%	**2.92%**	16.78%	3.52%
Li_30	1,040	9.04%	11.86%	**3.28%**	11.10%	4.46%
Li_31	1,120	11.53%	8.18%	3.47%	17.06%	**2.73%**
Li_32	1,200	9.40%	7.43%	**1.45%**	9.44%	3.41%
Leuven1	3,000	14.80%	15.39%	10.71%	14.95%	**3.54%**
Leuven2	4,000	22.82%	25.69%	21.22%	16.54%	**10.61%**
Antwerp1	6,000	11.66%	13.64%	8.91%	19.08%	**4.44%**
Antwerp2	7,000	16.27%	26.09%	15.42%	17.72%	**8.91%**
Ghent1	10,000	21.36%	OOM	17.28%	18.28%	**4.89%**
Ghent2	11,000	27.71%	OOM	25.77%	16.45%	**13.39%**
Brussels1	15,000	23.12%	OOM	OOM	26.17%	**6.26%**
Brussels2	16,000	34.87%	OOM	OOM	17.56%	**13.71%**
Flanders1	20,000	40.92%	OOM	OOM	24.02%	**6.90%**
Flanders2	30,000	129.81%	OOM	OOM	25.42%	**18.18%**
Sloved#		14/14	8/14	10/14	14/14	14/14
Avg.gap		27.07%	13.92%	11.04%	17.90%	**7.50%**

D.2 Result in Cross-Distributions

To evaluate robustness against distribution shifts, we tested TTPL on TSP and CVRP instances under three distinct spatial distributions (Clustered, Explosion, and Implosion)[15] on scales from 1,000 to 100,000 nodes.

Table 11: Solution length and runtimes for TSP and CVRP instances under Clustered, Explosion, and Implosion distributions.

	Clustered									
Method	TSP1K		TSP5K		TSP10K		TSP50K		TSP100K	
w/o proj	15.3	0.1s	35.4	1.4s	57.1	2.7s	185.6	13.5s	277.4	27.6s
seed proj	14.5	0.1s	29.8	1.5s	41.4	2.9s	91.0	14.6s	124.9	29.6s
TTPL	**14.4**	0.5s	**29.6**	3.2s	**41.3**	6.4s	**90.5**	33.9s	**123.9**	1.1m
	Explosion									
	TSP1K		TSP5K		TSP10K		TSP50K		TSP100K	
w/o proj	17.5	0.1s	39.0	1.3s	55.6	2.6s	193.6	13.5s	269.5	27.6s
seed proj	16.7	0.1s	34.1	1.5s	43.1	2.9s	88.4	14.6s	111.8	29.5s
TTPL	**16.4**	0.5s	**33.9**	3.2s	**42.4**	6.6s	**87.9**	34.1s	**110.9**	1.1m
	Implosion									
	TSP1K		TSP5K		TSP10K		TSP50K		TSP100K	
w/o proj	21.1	0.1s	52.5	1.3s	75.9	2.6s	212.0	13.5s	428.1	27.5s
seed proj	20.9	0.1s	**46.7**	1.5s	64.6	2.9s	141.6	14.5s	198.4	29.4s
TTPL	**20.7**	0.5s	46.7	3.2s	**64.2**	6.6s	**140.6**	33.8s	**196.8**	1.1m
	Clustered									
Method	CVRP-1K		CVRP-5K		CVRP-10K		CVRP-50K		CVRP-100K	
w/o proj	31.4	0.1s	87.4	1.7s	112.6	3.2s	433.6	16.5s	831.9	36.0s
seed proj	37.4	0.1s	90.3	1.7s	109.1	3.4s	217.7	17.2s	**373.7**	40.7s
TTPL	**31.1**	0.5s	**80.7**	3.8s	**93.8**	7.6s	**203.0**	39.3s	384.6	1.4m
	Explosion									
	CVRP-1K		CVRP-5K		CVRP-10K		CVRP-50K		CVRP-100K	
w/o proj	30.0	0.1s	70.2	1.6s	90.3	3.2s	401.3	16.5s	744.9	35.9s
seed proj	39.3	0.1s	78.4	1.7s	94.8	3.3s	203.7	17.2s	322.6	41.0s
TTPL	**29.6**	0.5s	**64.3**	3.8s	**75.5**	7.7s	**178.6**	39.1s	**294.4**	1.4m
	Implosion									
	CVRP-1K		CVRP-5K		CVRP-10K		CVRP-50K		CVRP-100K	
w/o proj	39.0	0.1s	102.6	1.6s	131.1	3.2s	402.4	16.5s	808.7	35.9
seed proj	51.5	0.1s	124.3	1.7s	149.6	3.3s	325.2	17.2s	549.7	41.7s
TTPL	**38.6**	0.5s	**98.2**	3.8s	**120.7**	7.7s	**299.0**	39.1s	**542.3**	1.4m

E Additional Experiment Analysis

E.1 Adaptability of TTPL

To further validate the effectiveness of TTPL framework, we utilize our proposed framework on different base models. Specifically, we compare POMO [7], LEHD [18], BQ [42], and SIGD [62], four **constructive** models, with and without TTPL projection. The test instances are set to TSP1K/5K/10K with the same settings as the previous. The results are shown in the Table. 12

E.2 TTPL Time Usage

To quantify the extra computational overhead introduced by the TTPL, we report the training time used for TTPL to search for a projection strategy in Table 13

E.3 Results from Other LLMs

To investigate the robustness of TTPL to different LLMs, we test our framework with several state-of-the-art LLMs, including Claude, Gemini, DeepSeek, and Qwen. The experimental results (Table 14) indicate that the choice of LLM does not significantly influence projection performance

Table 12: Results of different base models with and w/o TTPL

Method	TSP1K Obj.(Gap)	TSP5K Obj.(Gap)	TSP10K Obj.(Gap)
POMO greedy	33.18 (43.51%)	94.04 (84.50%)	150.64 (109.86%)
POMO-TTPL	**29.68 (28.37%)**	**71.76 (40.79%)**	**101.8 (41.82%)**
SIGD greedy	**23.57(1.96%)**	57.19 (12.20%)	93.80 (30.68%)
SIGD-TTPL	23.86 (3.20%)	**56.05 (9.97%)**	**80.44 (12.06%)**
BQ greedy	23.65 (2.30%)	58.27 (14.31%)	89.73 (25.02%)
BQ-TTPL	**23.58 (1.99%)**	**56.47(10.79%)**	**81.48 (13.51%)**
LEHD greedy	23.84 (3.11%)	58.85 (15.46%)	91.33 (27.24%)
LEHD-TTPL	**23.73 (2.65%)**	**52.63 (3.25%)**	**74.39 (3.63%)**

Table 13: Time used for TTPL to learn projection strategies on different scales

Mehod	TSP1K time	TSP5K time	TSP10K time
TTPL	5.5h	9.6h	19.9h

Table 14: Result of TTPL using different LLMs

Method	TSP1K Obj.	TSP5K Obj.	TSP10K Obj.
TTPL-Claude	23.80	52.79	74.48
TTPL-DeepSeek	23.67	52.39	74.00
TTPL-Gemini	23.76	53.71	76.42
TTPL-Qwen	23.75	52.73	74.25
TTPL-GPT-4o-mini	23.73	52.63	74.39

F Solution Visualization

## F.1 Solution Visualizations of Cross-distribution TSP Instances
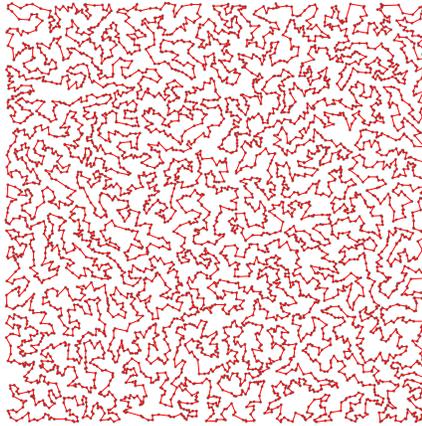
(a) Optimal solution.
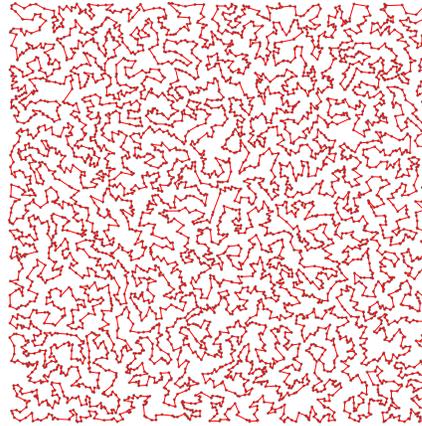
(b) TTPL aug RRC1000 (gap: 1.11%).

Figure 3: The solution visualizations of a TSP5K instance with uniform distribution.
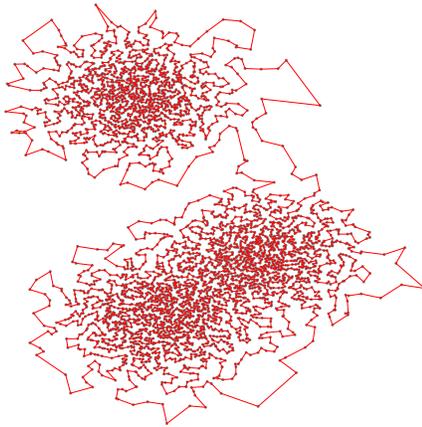

(a) Optimal solution.
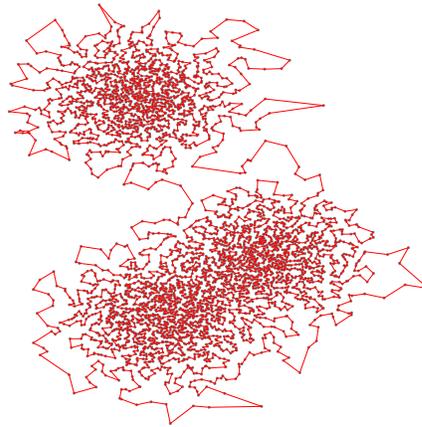
(b) TTPL aug RRC1000 (gap: 1.10%).

Figure 4: The solution visualizations of a TSP5K instance with cluster distribution.
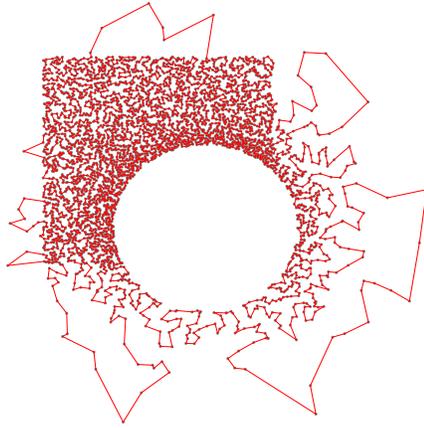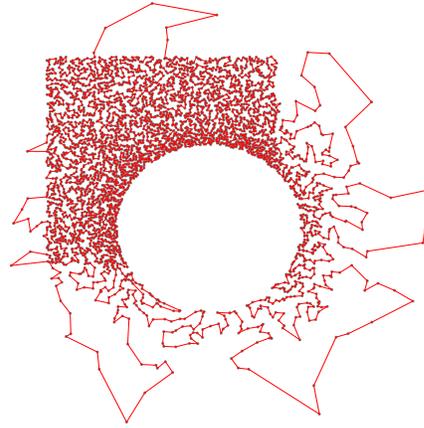
(a) Optimal solution.　　　　　(b) TTPL aug RRC1000 (gap: 0.94%).

Figure 5: The solution visualizations of a TSP5K instance with explosion distribution.
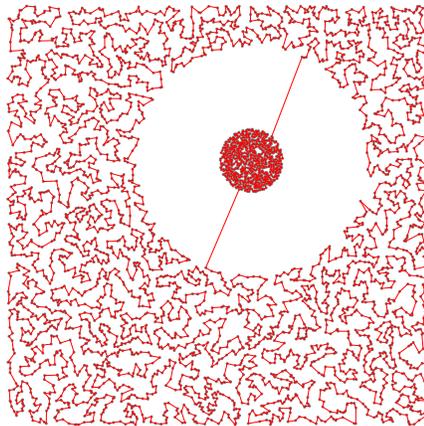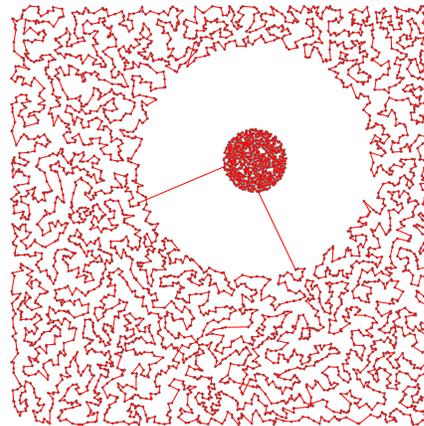
(a) Optimal solution.　　　　　(b) TTPL aug RRC1000 (gap: 1.56%).

Figure 6: The solution visualizations of a TSP5K instance with implosion distribution.

## F.2 Solution Visualizations of Large-scale TSPLIB Instances
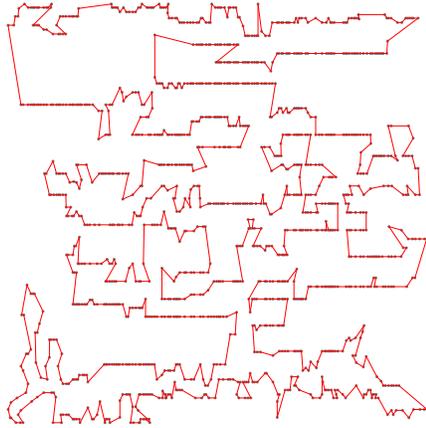
(a) Instance rl1304 (scale: 1304, gap: 0.12%.)
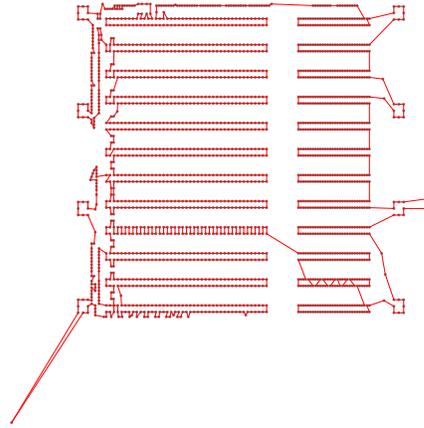
(b) Instance d2103 (scale: 2103, gap: 0.13%.)
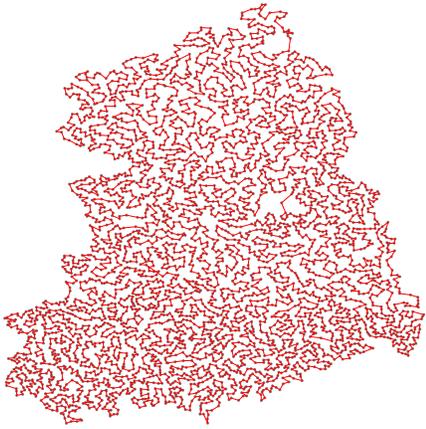
(c) Instance fnl4461 (scale: 4461, gap: 1.10%.)
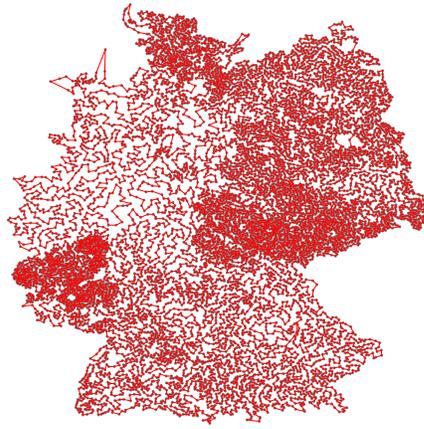
(d) Instance d15112 (scale: 15112, gap: 1.06%.)

Figure 7: The solution visualizations of TSPLIB[59] instances with different scales, the solutions are all generated by TTPL aug RRC1000.

G License

We list the license of the code and the dataset in the Table. 15.

Table 15: A summary of licenses

Resource	Type	Link	License
LKH3[57]	Code	http://webhotel4.ruc.dk/keld/research/LKH-3/	Available for academic research use
HGS[58]	Code	https://github.com/chkwon/PyHygese	MIT License
Concorde[82]	Code	https://github.com/jvkersch/pyconcorde	BSD 3-Clause License
POMO[7]	Code	https://github.com/yd-kwon/POMO	MIT License
LEHD[18]	Code	https://github.com/CIAM-Group/NCO_code/tree/main/ single_objective/LEHD	MIT License
BQ[42]	Code	https://github.com/naver/bq-nco	CC BY-NC-SA 4.0
GLOP[13]	Code	https://github.com/henry-yeh/GLOP	MIT License
H-TSP[12]	Code	https://github.com/Learning4Optimization-HUST/H-TSP	MIT License
DIFUSCO[28]	Code	https://github.com/Edward-Sun/DIFUSCO	MIT License
INViT[15]	Code	https://github.com/Kasumigaoka-Utaha/INViT	Available for academic research use
ELG[14]	Code	https://github.com/gaocrr/ELG	MIT License
SIGD[62]	Code	https://github.com/grimmlab/gumbeldore	Available for academic research use
EoH[52]	Code	https://github.com/FeiLiu36/EoH	MIT License
LLM4AD[83]	Code	https://github.com/Optima-CityU/LLM4AD	MIT License
TSPLIB[59]	Dataset	http://comopt.ifi.uni-heidelberg.de/software/TSPLIB95/	Available for any non-commercial use
CVRPLib[60]	Dataset	http://vrp.galgos.inf.puc-rio.br/index.php/en/	Available for academic research use

H Broader Impacts

This work advances neural combinatorial optimization through the proposed TTPL framework and MVFD technique, critically enhancing solution efficiency for large-scale Vehicle Routing Problems (VRPs). These developments are expected to inspire further investigations into novel neural methods for complex, large-scale routing tasks. We foresee no negative societal impacts from this research.